THE WAVE DRIFT DAMPING MATRIX AND APPLICATIONS

DESCRIPTION OF A COMPLETE THEORY AND
A PANEL PROGRAM FOR EVALUATION OF
WAVE-BODY INTERACTION INCLUDING
WAVE DRIFT DAMPING AND
RELATED QUANTITIES

John Grue and Styrk Finne

Mechanics Division
Department of Mathematics
University of Oslo

1999

CONTENTS

I. THEORY. DESCRIPTION OF THE LINEAR FORCES AND MOTIONS

The complete wave drift damping matrix and applications

Part 1: Description of the linear forces and motions

by

John Grue and Styrk Finne

Mechanics Division,
Department of Mathematics,
University of Oslo, Norway

CONTENTS

1 Introduction

This report summarises the first part of a method for obtaining the complete wave drift damping matrix. We consider a floating body which can perform linear oscillations in incoming waves, while drifting slowly horizontally in the surge, sway and yaw modes of motion, where the latter means a slow rotation about the vertical axis. The body may be moored by either tension legs or anchor lines. In this first part of the project report we describe how to obtain the various linear potentials, the linear forces and motions, and how the coupling between the waves and the slow horizontal motions is accounted for. The report is based on the publications in the reference list.

We apply potential theory to describe the fluid motion (see §2 & 3), as we disregard viscous effects and assume that the fluid is homogenous and incompressible. Furthermore, we use the powerful method of integral equations to compute the fluid flow. All parts of the method are obtained by strict mathematical procedures.

The derived integral equations contain unknown quantities on the wetted body surface only, which, among others, means that evaluation of only two coefficient matrices for linear systems are required, one for the wave part of the problem and one for the time-averaged part due to the slow motion. The set of perturbation potentials are then obtained by deriving a set of right hand sides of the equations which are used as input for the equation solver. The method requires evaluation of ordinary integrals over the mean free surface, which have relatively quick convergence and are relatively robust to evaluate. We employ a low-order panel method as numerical tool and use the midpoint rule for numerical integration, with exception of the singular integrals which are obtained by algoritms based on analytical methods. Convergence of the method is documented in several examples, and we have good reason to believe that the linear results and the wave drift damping matrix may be obtained with a relative accuracy within a few percents, depending on the discretization of the geometry.

In developing a rather complex method it is desirable to develop checks. This is part of our philosophy when we develop integral checks like the generalized Haskind relations, the generalized Timman-Newman relations (see §5) and the energy balance in the method. We show here numerical results for the two former relations which document the robustness and soundness of the method. (The energy check being second order in the wave amplitude is considered in a later report.) In §6 we briefly discuss the amplitudes and the frequencies of the linear body responses. We find among others that the different modes of motion in general have different frequencies, which is due to the slow rotation of the body. Furthermore we find that the frequency of the motion may differ from the frequency of the exciting force in the respective modes.

A code based on the mathematical formulation is under implementation as an extension of the WAMIT wave analysis program. The final wave drift damping (WDD) module contains a mixture between original WAMIT routines and new routines developed at UiO made adaptive to WAMIT. Roughly speaking, one third of the routines of the WDD-part are original from UiO; basically these are routines for the set of right hand sides due to the perturbation potentials, the set of auxillary (Green) functions due to a singularity with slow speed in waves, the wave forces, the motions and the wave drift damping due to the slow horizontal motions in waves. Another part consists of modified WAMIT-routines

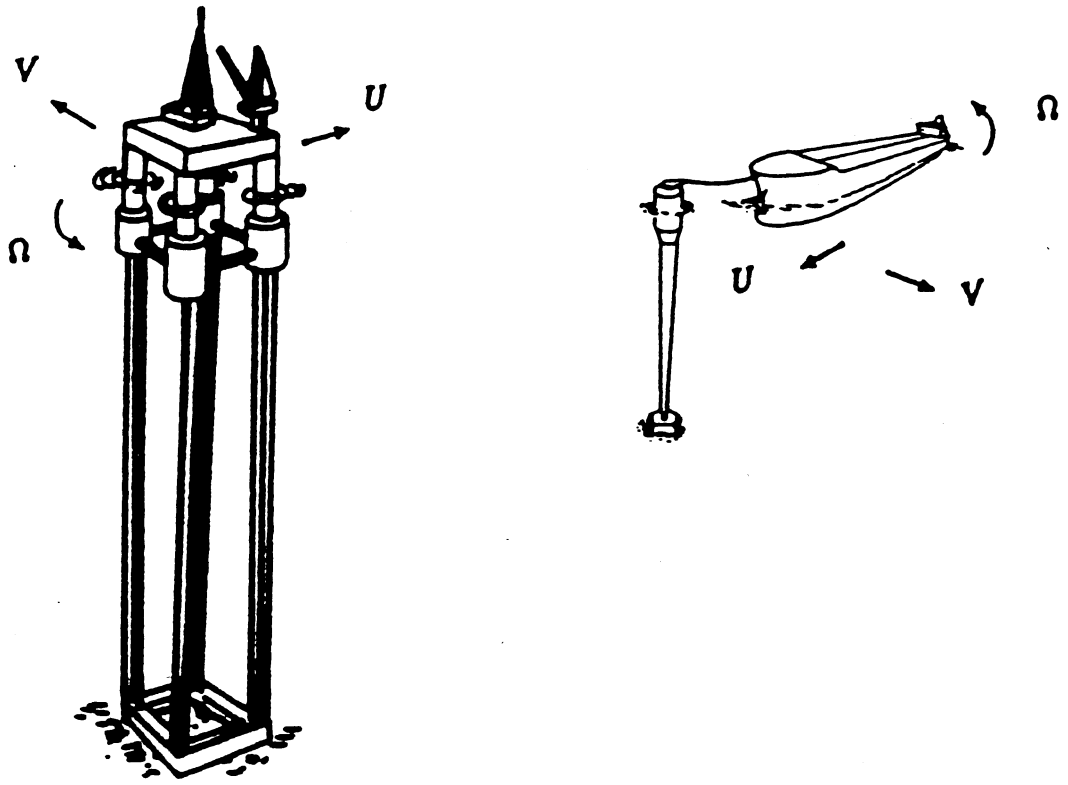

Figure 1: Sketch of floating offshore platform and ship. Slow velocities U, V and Ω are indicated.

(input/output, organization of panels, time-averaged problem), while a remaining part is original WAMIT-routines (evaluation of the coefficient matrices, equation solver, basic integration over a panel, zero speed Green function). The final wave drift damping program will be organized as a set of submodules fitted to the zero-speed WAMIT-program, where an index marks if the submodules for the WDD-part shall be included in a run. Otherwise the original zero-speed WAMIT program is run.

2 Mathematical formulation

We consider a floating body moving with slow velocities in the three horizontal modes of motion while being exposed to incoming monochromatic waves. We define a fixed frame of reference and a relative frame of reference where the latter follows the slow motion of the body, and is rotated an angle α relative to the fixed frame of reference. A coordinate system $O - xyz$ is introduced in the relative frame of reference with the xy-plane being in the mean free surface of the fluid, and the z-axis being vertical upwards. Unit vectors $\mathbf{i}, \mathbf{j}, \mathbf{k}$ are introduced accordingly. The slow velocity of the body, measured in the fixed frame of reference, is then given by $U\mathbf{i} + V\mathbf{j} + \Omega\mathbf{k}$, where $\Omega = \dot{\alpha}$ and a dot denotes time

derivative. We note that U, V and Ω are functions of time.

Let the incoming waves be described in the relative frame of reference by the potential

$$\Phi^I = Re[(Aig/\omega)\phi^I e^{i\sigma t}], \quad \phi^I = \frac{\cosh k(z+h)}{\cosh kh} e^{-ikR\cos(\beta-\theta)}, \tag{1}$$

where A, k and β denote wave amplitude, wavenumber and wave angle, respectively, of the incoming waves, h the water depth, and g the acceleration due to gravity. β is defined as the angle between the positive x-axis and the wave direction. The encounter frequency is given by

$$\sigma = \omega - Uk\cos\beta - Vk\sin\beta \tag{2}$$

where ω and k obey the dispersion relation

$$K = k\tanh kh \tag{3}$$

and $K = \omega^2/g$. In the incoming wave potential (1) we have also introduced polar coordinates by $x = R\cos\theta$, $y = R\sin\theta$.

The wave angle is constant and equal to β_0 in the fixed frame of reference. The slow rotation angle α of the body introduces effectively a slowly varying wave angle to an observer in the relative frame of reference. This wave angle is determined by $\beta(t) + \alpha(t) = \beta_0$, which means that

$$\frac{d\beta}{dt} = -\Omega. \tag{4}$$

The effect of a time-dependent wave angle will appear in the subsequent description.

We let the rotation angle α be of arbitrary magnitude and the non-dimensional wavenumber kl be of order one, where l denotes the characteristic length of the body. We further introduce the small parameters

$$\tau(U) = U\omega/g, \qquad \tau(V) = V\omega/g, \qquad \tau(\Omega) = \Omega/\omega. \tag{5}$$

In the mathematical analysis we apply perturbation expansions in the small parameters retaining terms up to order $(A/l)^2$, $\tau(U)$, $\tau(V)$ and $\tau(\Omega)$.

Let $\mathbf{v}$ denote the fluid velocity in the relative frame of reference. This velocity may be decomposed by

$$\mathbf{v} = \mathbf{v}' - U\mathbf{i} - V\mathbf{j} - \Omega\mathbf{k}\times\boldsymbol{x}, \tag{6}$$

where the latter three velocity components contribute to the velocity which is introduced to an observer which change his position from the fixed to the relative frame of reference. This also means that $\mathbf{v}'$ denotes the velocity in the fixed frame of reference.

We assume that $\mathbf{v}'$ can be described by a Laplacian velocity potential Φ'. It is convenient to decompose this potential by

$$\Phi' = \Phi + U\chi^U + V\chi^V + \Omega\chi^\Omega + \psi^{(2)}. \tag{7}$$

Here, Φ denotes the linear wave potential being proportional to the wave amplitude and is due to the incoming, scattered and radiated waves, $U\chi^U + V\chi^V + \Omega\chi^\Omega$ the potential

due to the flow generated by the body when there are no waves, and $\psi^{(2)}$ a time-averaged potential being proportional to the wave amplitude squared. For later use it is convenient to define the following set of velocities:

$$\mathbf{w} = U\mathbf{w}^U + V\mathbf{w}^V + \Omega\mathbf{w}^\Omega, \tag{8}$$

where

$$\mathbf{w}^U = -\mathbf{i} + \nabla\chi^U, \tag{9}$$
$$\mathbf{w}^V = -\mathbf{j} + \nabla\chi^V, \tag{10}$$
$$\mathbf{w}^\Omega = -\mathbf{k} \times \boldsymbol{x} + \nabla\chi^\Omega. \tag{11}$$

The velocities in (9)–(11) satisfy the rigid wall boundary condition at the body, at the free surface and at the sea floor, and χ^U, χ^V, χ^Ω vanish at infinity.

3 Boundary value problems

The free surface boundary condition for the wave potential Φ is obtained by applying the individual derivative to the Bernoulli equation for the pressure at the free surface. After linearizing with respect to the wave amplitude, we find (see references 3, 11, 12)

$$\Phi_{tt} + 2\mathbf{w} \cdot \Phi_t + \Phi_t \nabla_h \cdot \mathbf{w} + g\Phi_z = 0 \text{ at } z = 0, \tag{12}$$

where ∇_h denotes the horizontal gradient.

We next introduce the following decomposition of the velocity potential

$$\Phi = Re\Big((iAg/\omega)\phi_D e^{i\sigma t} + \sum_{j=1}^{6} \frac{d}{dt}(\xi_j e^{i\sigma t})\phi_j\Big), \tag{13}$$

where the first part represents the incoming and scattered waves, and the second part the radiation potential. ξ_j denotes the amplitude of oscillation in mode j ($j = 1, ..., 6$). As noted above, the motion in the relative frame of reference depend on the slowly varying wave angle $\beta(t)$. This means that e.g.

$$\frac{d}{dt}(\xi_j e^{i\sigma t}) = (i\sigma\xi_j - \Omega\frac{\partial \xi_j}{\partial \beta})e^{i\sigma t}, \quad j = 1, ..., 6, \tag{14}$$

$$\frac{\partial}{\partial t}(\phi_j e^{i\sigma t}) = (i\sigma\phi_j - \Omega\frac{\partial \phi_j}{\partial \beta})e^{i\sigma t}, \quad j = 1, ..., 6, D, \tag{15}$$

where we have used that $d\beta/dt = -\Omega$. We now introduce the expansions

$$\xi_j = \xi_j^0 + \tau(U)\xi_j^{1U} + \tau(V)\xi_j^{1V} + \tau(\Omega)\xi_j^{1\Omega}, \quad j = 1, ..., 6, \tag{16}$$
$$\phi_D = \phi_D^0 + \tau(U)\phi_D^{1U} + \tau(V)\phi_D^{1V} + \tau(\Omega)\phi_D^{1\Omega}, \tag{17}$$
$$\xi_j\phi_j = \xi_j^0\phi_j^0 + \tau(U)(\xi_j\phi_j)^{1U} + \tau(V)(\xi_j\phi)^{1V} + \tau(\Omega)(\xi_j\phi_j)^{1\Omega}, \quad j = 1, ..., 6, \tag{18}$$

where

$$(\xi_j\phi_j)^{1U} = \xi_j^0\phi_j^{1U} + \xi_j^{1U}\phi_j^0, \tag{19}$$

$$(\xi_j\phi_j)^{1V} = \xi_j^0\phi_j^{1U} + \xi_j^{1U}\phi_j^0, \tag{20}$$

$$(\xi_j\phi_j)^{1\Omega} = \xi_j^0\psi_j^{1\Omega} + \frac{\partial\xi_j^0}{\partial\beta}\phi_j^{11\Omega} + \xi_j^{1\Omega}\phi_j^0. \tag{21}$$

Here, ϕ_D^0, ϕ_j^0, ξ_j^0 are the usual linear zero-speed potentials and motions. The quantities ϕ_D^{1U}, ϕ_j^{1U}, ξ_j^{1U} are required to account for couplings between the waves and the slow speed U, likewise, ϕ_D^{1V}, ϕ_j^{1V}, ξ_j^{1V} are required to account for the speed V, and finally, $\phi_D^{1\Omega}$, $\psi_j^{1\Omega}$, $\phi_j^{11\Omega}$, $\xi_j^{1\Omega}$, $\partial\xi_j^0/\partial\beta$ are required to include the effect of a slow rotation.

The zero-speed potentials satisfy the following set of boundary value problems

$$-K\phi_j^0 + \frac{\partial\phi_j^0}{\partial z} = 0 \quad \text{at} \quad z = 0, \tag{22}$$

$$\frac{\partial\phi_j^0}{\partial n} = \begin{cases} n_j, & j = 1, ..., 6, \\ 0, & j = D, \end{cases} \tag{23}$$

$$\phi_j^0 - \phi^I\delta_{jD} = R^{-1/2}H_j^0(\theta)\frac{\cosh k(z+h)}{\cosh kh}e^{-ikR} + O(1/R), \quad R \to \infty, \tag{24}$$

where δ_{jD} denotes the Kroenecker delta, $(n_1, n_2, n_3) = \mathbf{n}$ the unit normal at the floating body pointing out of the fluid, $(n_4, n_5, n_6) = \boldsymbol{x} \times \mathbf{n}$ and $H_j^0(\theta)$ the far-field amplitude of the respective potential. We also have that $\partial\phi_j^0/\partial z = 0$ at $z = -h$.

3.1 The perturbation potentials

We next consider the perturbation potentials. At the free surface ($z = 0$) they satisfy (see references 3, 11, 12, 13)

$$-K\phi_j^{1U} + \frac{\partial\phi_j^{1U}}{\partial z} = -2k\cos\beta\phi_j^0 + 2i\frac{\partial\phi_j^0}{\partial x} - iL_h(\phi_j^0, \chi^U), \quad j = 1, ..., 6, D, \tag{25}$$

$$-K\phi_j^{1V} + \frac{\partial\phi_j^{1V}}{\partial z} = -2k\sin\beta\phi_j^0 + 2i\frac{\partial\phi_j^0}{\partial y} - iL_h(\phi_j^0, \chi^V), \quad j = 1, ..., 6, D, \tag{26}$$

$$-K\phi_D^{1\Omega} + \frac{\partial\phi_D^{1\Omega}}{\partial z} = 2iK\frac{\partial\phi_D^0}{\partial\beta} + 2iK\frac{\partial\phi_D^0}{\partial\theta} - iKL_h(\phi_D^0, \chi^\Omega), \tag{27}$$

$$-K\psi_j^{1\Omega} + \frac{\partial\psi_j^{1\Omega}}{\partial z} = 2iK\frac{\partial\phi_j^0}{\partial\theta} - iKL_h(\phi_j^0, \chi^\Omega), \quad j = 1, ..., 6, \tag{28}$$

$$-K\phi_j^{11\Omega} + \frac{\partial\phi_j^{11\Omega}}{\partial z} = 2iK\phi_j^0, \quad j = 1, ..., 6, \tag{29}$$

where $L_h(\phi, \chi) = 2\nabla_h\phi \cdot \nabla_h\chi + \phi\nabla_h^2\chi$.

Furthermore, the kinematic boundary condition at the body gives

$$\frac{\partial\phi_j^{1s}}{\partial n} = \begin{cases} -im_j^s/K, & j = 1, ..., 6, \ s = U, V, \\ 0, & j = D, \ s = U, V, \end{cases} \tag{30}$$

$$\frac{\partial \psi_j^{1\Omega}}{\partial n} = \begin{cases} -im_j^{\Omega}, & j = 1, ..., 6, \\ 0, & j = D, \end{cases} \tag{31}$$

$$\frac{\partial \phi_j^{11\Omega}}{\partial n} = 0, \tag{32}$$

where

$$(m_1, m_2, m_3)^s = -\mathbf{n} \cdot \nabla \mathbf{w}^s, \quad s = U, V, \tag{33}$$

$$(m_4, m_5, m_6)^s = -\mathbf{n} \cdot \nabla (\boldsymbol{x} \times \mathbf{w}^s), \quad s = U, V, \tag{34}$$

$$(m_1, m_2, m_3)^{\Omega} = -\mathbf{n} \cdot \nabla \mathbf{w}^{\Omega} - 2\mathbf{k} \times \mathbf{n}, \tag{35}$$

$$(m_4, m_5, m_6)^{\Omega} = -\mathbf{n} \cdot \nabla (\boldsymbol{x} \times \mathbf{w}^{\Omega}) - 2\boldsymbol{x} \times (\mathbf{k} \times \mathbf{n}). \tag{36}$$

We note that m_j^{Ω} include some new terms introduced due to the slow rotation of the body, given by

$$-2\mathbf{k} \times \mathbf{n}, \tag{37}$$

$$-2\boldsymbol{x} \times (\mathbf{k} \times \mathbf{n}). \tag{38}$$

These terms are absent in the translatory modes of motion.

There is also a radiation condition for the flow when the incoming wave-field is subtracted. The radiation condition requires that all disturbances due to the presence of the body in the far-field behave as outgoing waves only. This is equivalent to requiring that there are no energy sources as $R \to \infty$, except the incoming waves. For the potentials due to U and V we find (see references 3, 9)

$$\phi_j^0 - \phi^I \delta_{jD} + \tau(U)\phi^{1U} = R^{-1/2} H_j^U(\theta) \frac{\cosh k^{1U}(z+h)}{\cosh k^{1U} h} e^{-ik^{1U}R} + O(1/R), \quad R \to \infty, \tag{39}$$

$$\phi_j^0 - \phi^I \delta_{jD} + \tau(V)\phi^{1V} = R^{-1/2} H_j^V(\theta) \frac{\cosh k^{1V}(z+h)}{\cosh k^{1V} h} e^{-ik^{1V}R} + O(1/R), \quad R \to \infty, \tag{40}$$

where

$$k^{1U} = k\Big(1 + \frac{2\tau(U)}{C_g(kh)}(\cos\theta - \cos\beta)\Big), \tag{41}$$

$$k^{1V} = k\Big(1 + \frac{2\tau(V)}{C_g(kh)}(\sin\theta - \sin\beta)\Big), \tag{42}$$

$$C_g(kh) = \tanh kh + \frac{kh}{\cosh^2 kh} \tag{43}$$

and $H_j^{U,V}$ denote far-field amplitudes of the potentials.

In the slow yaw-problem we obtain the potentials as follows, see references 11–13,

$$\phi_D^{1\Omega} = 2iK \frac{\partial^2 \phi_D^0}{\partial K \partial \beta} + 2iK \frac{\partial^2 \phi_D^0}{\partial K \partial \theta} + \phi_D^{13\Omega}, \tag{44}$$

$$\psi_j^{1\Omega} = 2iK \frac{\partial^2 \phi_j^0}{\partial K \partial \theta} + \phi_j^{13\Omega}, \quad j = 1, ..., 6, \tag{45}$$

$$\phi_j^{11\Omega} = 2iK \frac{\partial \phi_j^0}{\partial K}, \quad j = 1, ..., 6, \tag{46}$$

where $\phi_j^{13\Omega}$ satisfy

$$\phi_j^{13\Omega} = R^{-1/2} H_j^{13\Omega}(\theta) \frac{\cosh k(z+h)}{\cosh kh} e^{-ikR} + O(1/R), \quad R \to \infty, \quad j = 1, ..., 6, D \tag{47}$$

and $H_j^{13\Omega}$ denotes the far-field amplitude of $\phi_j^{13\Omega}$.

In addition, the perturbation potentials satisfy the rigid wall boundary condition at the sea floor.

The various potentials are determined numerically by means of integral equations. First we find the zero speed potentials ϕ_j^0 at the body surface and the free surface. Next we determine the potentials χ^U, χ^V and χ^Ω by applying source distributions. We then determine the potentials ϕ_j^{1U}, ϕ_j^{1V}, $\phi_D^{1\Omega}$, $\psi_j^{1\Omega}$, $\phi_j^{11\Omega}$ on the wetted body surface. The integral equations for the latter potentials are obtained by application of Green's theorem to the respective potentials, the zero speed Green function and certain derivatives of the zero speed Green function. Formal derivations of the integral equations for ϕ_j^0, ϕ_j^{1U}, ϕ_j^{1V}, are given in the references 3, 9, and for $\phi_D^{1\Omega}$, $\psi_j^{1\Omega}$, $\phi_j^{11\Omega}$, in the references 11, 12, 13. The results are

ϕ_j^0:

$$\int_{S_B} \phi_D^0 G_n^0 dS - 4\pi\phi^I = \begin{cases} -2\pi\phi_D^0(\boldsymbol{x}) \\ -4\pi\phi_D^0(\boldsymbol{x}), \end{cases} \tag{48}$$

$$\int_{S_B} (\phi_j^0 G_n^0 - G^0 n_j) dS = \begin{cases} -2\pi\phi_j^0(\boldsymbol{x}) \\ -4\pi\phi_j^0(\boldsymbol{x}). \end{cases} \tag{49}$$

ϕ_j^{1U}:

$$\int_{S_B} (\phi_D^{1U} G_n^0 - \phi_D^0 G_n^{1U} + \phi_D^0 2k\cos\beta G_{Kn}^0) dS$$
$$-i\int_{S_F} \phi_D^0 L_h(G^0, \chi^U) dS = \begin{cases} -2\pi\phi_D^{1U}(\boldsymbol{x}) \\ -4\pi\phi_D^{1U}(\boldsymbol{x}), \end{cases} \tag{50}$$

$$\int_{S_B} (\phi_j^{1U} G_n^0 - \frac{i}{K}\mathbf{w}^U \cdot \nabla G^0 n_j - \phi_j^0 G_n^{1U} + \phi_j^0 2k\cos\beta G_{Kn}^0 + G^{1U} n_j) dS$$
$$-i\int_{S_F} \phi_j^0 L_h(G^0, \chi^U) dS = \begin{cases} -2\pi\phi_j^{1U}(\boldsymbol{x}) \\ -4\pi\phi_j^{1U}(\boldsymbol{x}), \end{cases} \tag{51}$$

where S_B denotes the wetted body surface, S_F the free surface and $(\ )_n = \partial/\partial n$. The equations for ϕ_j^{1V} are similar.

$\psi_j^{1\Omega}$:

$$\int_{S_B} (\phi_D^{1\Omega} G_n^0 - \phi_D^0 G_n^{1\Omega} - 2iK\frac{\partial\phi_D^0}{\partial\beta} G_{Kn}^0) dS$$
$$-iK\int_{S_F} \phi_D^0 L_h(G^0, \chi^\Omega) dS = \begin{cases} -2\pi\phi_D^{1\Omega}(\boldsymbol{x}) \\ -4\pi\phi_D^{1\Omega}(\boldsymbol{x}), \end{cases} \tag{52}$$

$$\int_{S_B}(\psi_j^{1\Omega}G_n^0 - i\mathbf{w}^\Omega\cdot\nabla G^0 n_j - \phi_j^0 G_n^{1\Omega} + G^{1\Omega}n_j)dS$$

$$-iK\int_{S_F}\phi_j^0 L_h(G^0,\chi^\Omega)dS = \begin{cases} -2\pi\psi_j^{1\Omega}(\boldsymbol{x}) \\ -4\pi\psi_j^{1\Omega}(\boldsymbol{x}). \end{cases} \tag{53}$$

In the first cases of (48)–(53), $\boldsymbol{x}\in S_B$, which determines the respective potentials at S_B. For the latter cases, $\boldsymbol{x}$ is in the fluid volume, which determines the potentials in the fluid. $\phi_j^{11\Omega}$ may be obtained by differentiating (49) with respect to K.

The Green function G^0, being a source at $\boldsymbol{x}=\boldsymbol{\xi}'=(\xi',\eta',\zeta')$, is given by (see reference 14, eq. 13.18)

$$G^0(\boldsymbol{x},\boldsymbol{\xi}) = \frac{1}{r_1}+\frac{1}{r_2}+\Psi(\boldsymbol{x},\boldsymbol{\xi}') \tag{54}$$

where

$$r_1 = \sqrt{(x-\xi')^2+(y-\eta')^2+(z-\zeta')^2}, \tag{55}$$

$$r_2 = \sqrt{(x-\xi')^2+(y-\eta')^2+(z+\zeta'+2h)^2}, \tag{56}$$

$$\Psi(\boldsymbol{x},\boldsymbol{\xi}) = \frac{1}{2\pi}\int_0^{2\pi}\int_0^\infty \frac{2e^{-vh}(K+v)}{\cosh vh(v\tanh vh-K)}\cosh v(\zeta'+h)\cosh v(z+h)$$

$$\times e^{iv((x-\xi')\cos\alpha+(y-\eta')\sin\alpha)}dvd\alpha \tag{57}$$

and the integration is above the pole at $v\tanh vh - K = 0$. The auxillary functions are

$$G^{1U} = 2i\frac{\partial^2 G^0}{\partial\xi'\partial K}, \tag{58}$$

$$G^{1V} = 2i\frac{\partial^2 G^0}{\partial\eta'\partial K}, \tag{59}$$

$$G^{1\Omega} = 2iK\frac{\partial^2 G^0}{\partial\theta'\partial K} \tag{60}$$

and $\theta' = \tan^{-1}(\eta'/\xi')$.

4 The pressure. Free surface elevation

The linear pressure in the fluid is given by the Bernoulli equation and may be written

$$-\frac{p}{\rho} = \frac{\partial\Phi}{\partial t} + (U\mathbf{w}^U + V\mathbf{w}^V + \Omega\mathbf{w}^\Omega)\cdot\nabla\Phi + gz \tag{61}$$

where p and ρ denote pressure and density of the fluid, respectively.

The free surface elevation $\zeta(x,y,t)$ is determined from (61) by setting the pressure equal to zero at $z=\zeta$, giving for the linear part

$$g\zeta = -\frac{\partial\Phi}{\partial t} - (U\mathbf{w}^U + V\mathbf{w}^V + \Omega\mathbf{w}^\Omega)\cdot\nabla\Phi \quad \text{at } z=0 \tag{62}$$

5 The linear forces

5.1 The exciting force

The exciting force and moment are obtained by pressure integration over the body. By setting $\xi_j = 0$ we obtain

$$F_j = -\rho \int_{S_B} (\frac{\partial \Phi}{\partial t} + \mathbf{w} \cdot \nabla \Phi) n_j dS = Re(A e^{i\sigma t} X_j), \quad j = 1, ..., 6. \tag{63}$$

It is appropriate to expand the components of X_j by

$$X_j = X_j^0 + \tau(U) X_j^{1U} + \tau(V) X_j^{1V} + \tau(\Omega) X_j^{1\Omega}. \tag{64}$$

The exciting force and moment are then found by integrating the diffraction potential and the product between the velocity $\mathbf{w}$ and the gradient of the zero speed diffraction potential over the body surface. This results in a simple procedure once the diffraction potential and the source distributions for $\mathbf{w}$ and ϕ_D^0 are determined (we also find ϕ_j^0 by source distributions in order to evaluate $\nabla \phi_j^0$).

As an alternative to pressure integration we develop generalized Haskind relations for the components of the exciting force. This means that we are expressing component number j of the exciting force by the far-field amplitude of the radiation potential in mode number j. These relations constitute quite remarkable connections between the diffraction and the radiation problems. The relations for zero speed are well known and may be written as

$$\frac{X_j^0}{\rho g} = \sqrt{\frac{2\pi}{k}} C_g(kh) H_j^0(\beta + \pi) e^{i\pi/4}, \quad j = 1, ..., 6, \tag{65}$$

where $H_j^0(\beta + \pi)$ denotes the far-field amplitude of the potential ϕ_j^0, see eq. (24).

Extensions of the Haskind relations to also include slow horizontal speeds are non-trivial and require a set of mathematical manipulations. In short, we apply Green's theorem and the boundary conditions for the potentials involved, and in addition some mathematical tricks, see references 3, 9, 13. The final results are ($j = 1, ..., 6$)

$$\frac{X_j^{1U}}{\rho g} = -\sqrt{\frac{2\pi}{k}} C_g(kh) \Big(\frac{k}{K} \cos\beta H_j^0(\beta + \pi) + H_j^{13U}(\beta + \pi) \Big) e^{i\pi/4}, \tag{66}$$

$$\frac{X_j^{1V}}{\rho g} = -\sqrt{\frac{2\pi}{k}} C_g(kh) \Big(\frac{k}{K} \sin\beta H_j^0(\beta + \pi) + H_j^{13V}(\beta + \pi) \Big) e^{i\pi/4}, \tag{67}$$

$$\frac{X_j^{1\Omega}}{\rho g} = -\sqrt{\frac{2\pi}{k}} C_g(kh) \Big(i \frac{\partial H_j^0}{\partial \beta}(\beta + \pi) + H_j^{13\Omega}(\beta + \pi) \Big) e^{i\pi/4}, \tag{68}$$

where

$$4\pi H_j^{13U}(\theta) = -\int_{S_B} [(\psi_j^{1U} - 2k\cos\theta \phi_{jK}^0) h_n^0 - \frac{i}{K} \nabla h^0 \cdot \mathbf{w}^U n_j] dS + i \int_{S_F} \phi_j^0 L_h(h^0, \chi^U) dS, \tag{69}$$

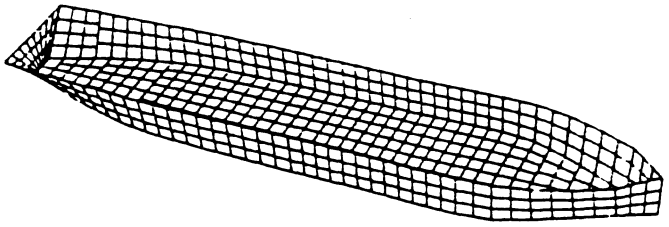

Figure 2: Geometry of a TPS.

$$4\pi H_j^{13V}(\theta) = -\int_{S_B}[(\psi_j^{1V} - 2k\sin\theta\phi_{jK}^0)h_n^0 - \frac{i}{K}\nabla h^0\cdot\mathbf{w}^V n_j]dS + i\int_{S_F}\phi_j^0 L_h(h^0,\chi^V)dS, \quad (70)$$

$$4\pi H_j^{13\Omega}(\theta) = -\int_{S_B}(\psi_j^{1\Omega}h_n^0 - 2iK\phi_{jK}^0 h_{\theta n}^0 - i\nabla h^0\cdot\mathbf{w}^\Omega n_j)dS + iK\int_{S_F}\phi_j^0 L_h(h^0,\chi^\Omega)dS, \quad (71)$$

$$h^0 = \frac{\sqrt{2\pi k}}{C_g(kh)}\big(\tanh kh + 1\big)\big(e^{k\zeta'} + e^{-k(\zeta'+2h)}\big)e^{k(i\xi'\cos\theta + i\eta'\sin\theta) - i\pi/4} \quad (72)$$

and $L_h(h,\chi)$ is given after equation (29). Furthermore, $\psi_j^{1V} = \phi_j^{1V} + 2k\cos\beta\phi_{jK}^0$, $\psi_j^{1V} = \phi_j^{1V} + 2k\sin\beta\phi_{jK}^0$.

Examples for the exciting force due to a body in translatory motion (U,V) is obtained earlier, see references 3, 4, 9, and confirm the generalized Haskind relations for translation. Here we show one example for X_j^{1U} from reference 3, where the geometry is a half-immersed sphere, see figure 3.

In the next example we show the exciting force on a ship in slow rotation. As ship geometry we choose a vessel oriented along the x-axis with section given by a half-circle and beam

$$B(x) = B_0[1 - (2x/l)^4], \quad |x| < l/2, \quad (73)$$

where l denotes the ship length and the ratio l/B_0 is 5.6. We hereafter refer to this geometry as ship 1. The dimensions of ship 1 correspond to the dimensions of a Turret Production Ship (TPS) which is considered in some examples later (see figure 2). Working with the geometry (73) is advantagous, since refinement of the discretization and thereby convergence tests are relatively easy to perform. In figure 4 we show $X_j^{1\Omega}$ in heave and pitch for ship 1 for two different wave angles, viz. $\beta = 135°$ (quartering seas) and $\beta = 157°$. $X_j^{1\Omega}$ is obtained by both pressure integration and the generalized Haskind relation, with good agreement between the two different methods.

For comparison we also show in figure 4 the corresponding components of the exciting force for $U = V = \Omega = 0$, illustrating that $|X_j^{1\Omega}| >> |X_j^0|$ in these examples.

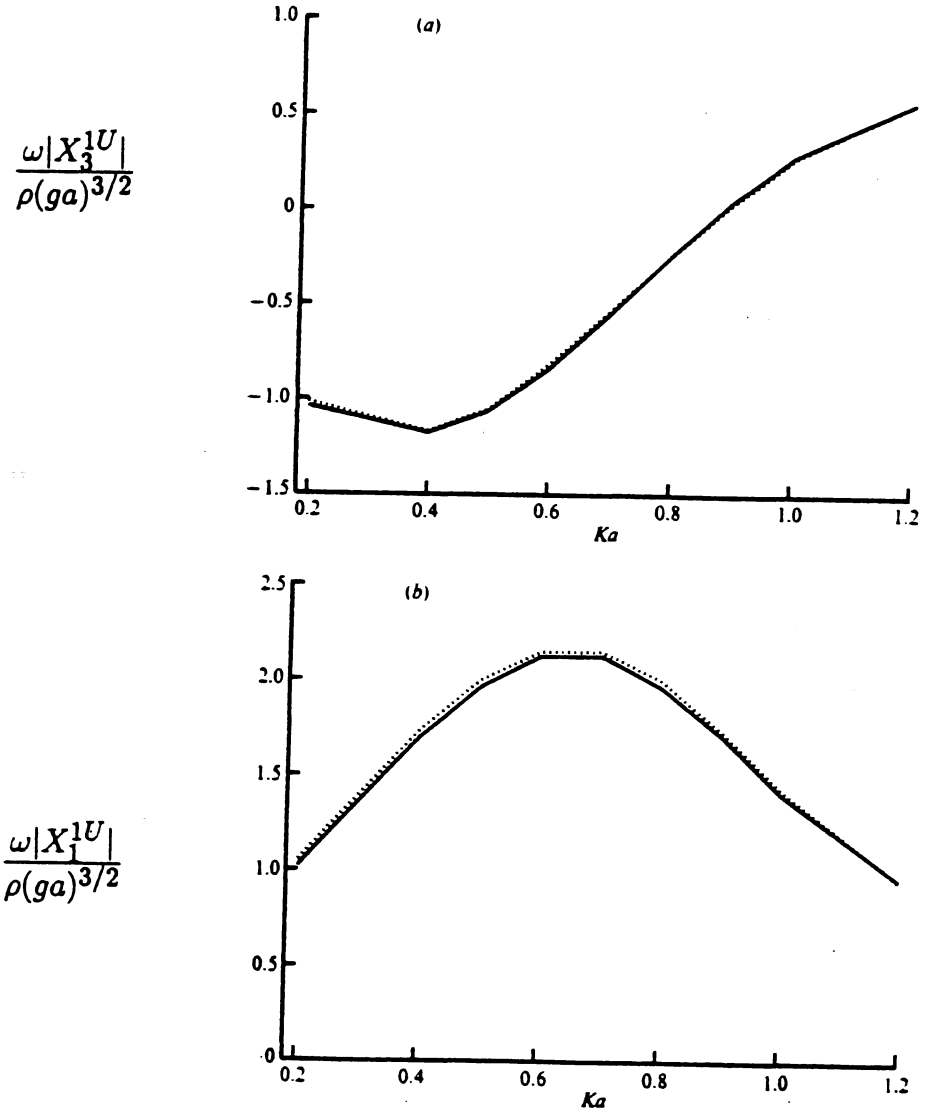

Figure 3: Exciting force $|X_j^{1U}|$ in heave (a) and surge (b) for a half-immersed sphere with radius a. $h = \infty$. $\beta = 180°$. Solid line: Pressure integration. Dotted line: Generalized Haskind relation. 400 panels on S_B, 880 panels on S_F.

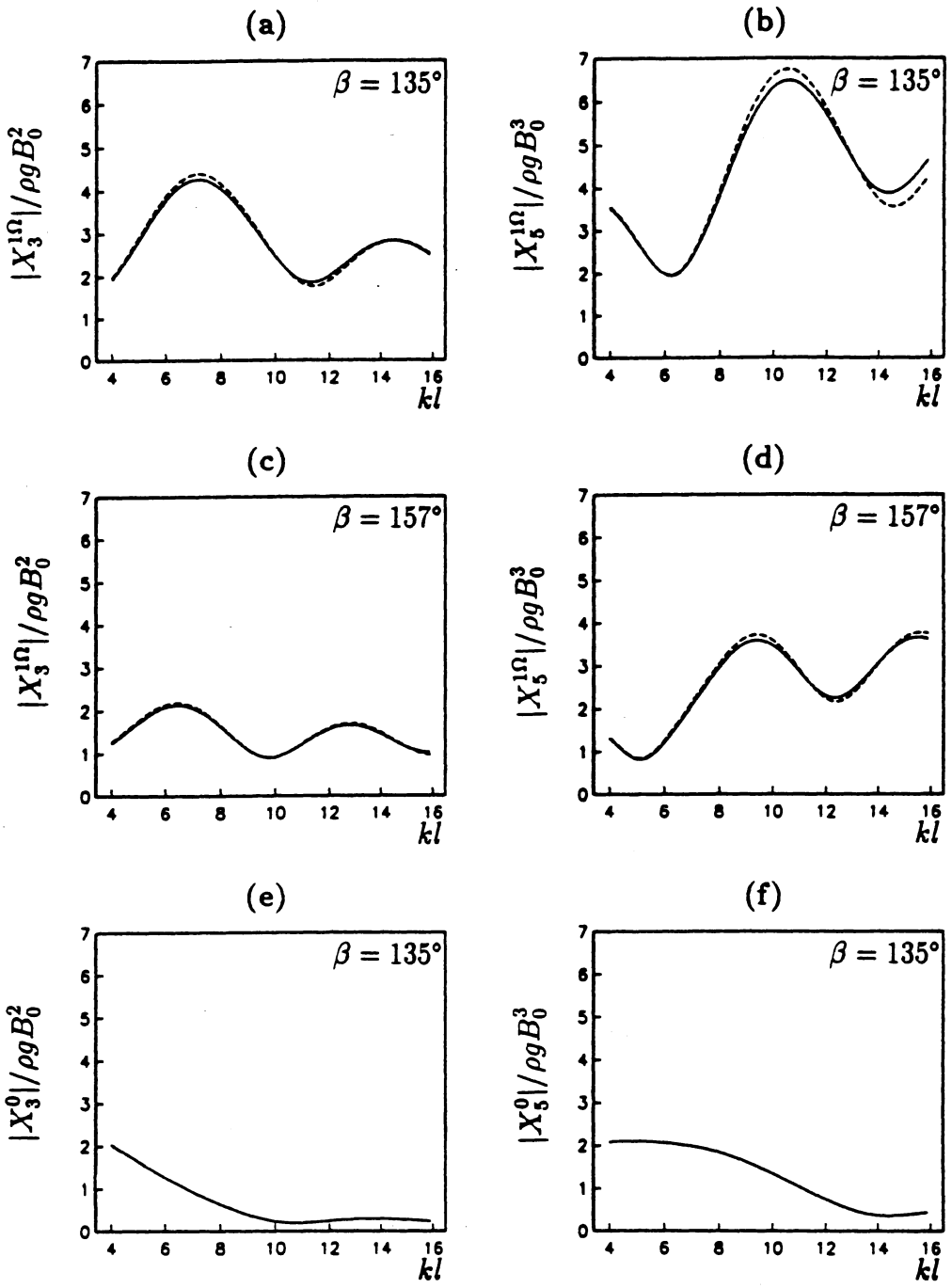

Figure 4: Exciting force $|X_j^{1\Omega}|$ in heave and pitch for ship 1. Solid line: Generalized Haskind relations. Dashed line: Pressure integration. (a)-(b): $\beta = 135°$. (c)-(d): $\beta = 157°$. (e)-(f): $|X_j^0|$. $h = \infty$. 1568 panels on S_B, 6272 panels on S_F.

5.2 Added mass and damping

By next setting the wave amplitude equal to zero ($A = 0$) we obtain the pressure force and moment in the radiation problem

$$F_j = -\rho \int_{S_B} (\frac{\partial \Phi}{\partial t} + \mathbf{w} \cdot \nabla \Phi) n_j dS = Re(\sigma^2 e^{i\sigma t} \sum_{k=1}^{6} \xi_k f_{jk}), \quad j = 1, ..., 6, \tag{74}$$

where the coefficients f_{jk} contain the added mass and damping forces. These forces are found by integrating the pressure due to the radiation potentials over the body surface, which is a quite simple procedure once the radiation potentials are determined. Due to the slow motion of the body we also get a coupling between the velocity $\mathbf{w}$ and the gradient of the zero speed radiation potentials.

It is convenient to expand $\xi_j f_{jk}$ by

$$\begin{aligned}
\xi_j f_{jk} = {} & \xi_j^0 f_{jk}^0 \\
& + \tau(U)(\xi_j^0 f_{jk}^{1U} - 2k \cos\beta \xi_j^0 \frac{\partial}{\partial K}(f_{jk}^0) + \xi_j^{1U} f_{jk}^0) \\
& + \tau(V)(\xi_j^0 f_{jk}^{1V} - 2k \sin\beta \xi_j^0 \frac{\partial}{\partial K}(f_{jk}^0) + \xi_j^{1V} f_{jk}^0) \\
& + \tau(\Omega)(\xi_j^0 f_{jk}^{1\Omega} + 2i \frac{\partial \xi_j^0}{\partial \beta} \frac{\partial}{\partial K}(K f_{jk}^0) + \xi_j^{1\Omega} f_{jk}^0).
\end{aligned} \tag{75}$$

For unidirectional forward speed, neglecting the χ^U-field, Timman and Newman showed for a slender ship that

$$f_{jk}^0 = f_{kj}^0, \qquad f_{jk}^{1U} = -f_{kj}^{1U}. \tag{76}$$

The Timman-Newman relations may be extended to the slow drift case for geometries of arbitrary shape, and with the χ^U, χ^V, χ^Ω-fields included. The extended results are proved by using Green's theorem and the boundary conditions for the potentials involved, see references 3, 9, 13. We find

$$f_{ij}^{1s} = -f_{ji}^{1s}, \quad s = U, V, \Omega. \tag{77}$$

In figure 5 is shown an example from reference 3 for the added mass and damping in translation, illustrating quite well the antisymmetry of f_{ij}^{1U}.

In the next examples we consider $f_{ij}^{1\Omega}$ due to slow rotation of ship 1 and the TPS (model shown in figure 2), more precisely the cross-coupling coefficients between sway and pitch, $f_{25}^{1\Omega}$, $-f_{52}^{1\Omega}$, and between heave and yaw, $f_{36}^{1\Omega}$, $-f_{63}^{1\Omega}$, see figure 6. The numerical results illustrate that $f_{ij}^{1\Omega} \simeq -f_{ji}^{1\Omega}$, in agreement with the theory. The results for $f_{25}^{1\Omega}$, $f_{52}^{1\Omega}$ are quite similar for the two ships, in spite of their quite different geometries.

While the zero speed cross-coupling coefficients f_{35}^0, f_{53}^0 are different from zero for the TPS, the cross-coupling coefficients $f_{35}^{1\Omega}$, $f_{53}^{1\Omega}$ in rotation are zero for this ship. For ship 1, being symmetric also with respect to $x = 0$, we have $f_{35}^0 = f_{53}^0 = f_{35}^{1\Omega} = f_{53}^{1\Omega} = 0$ in all the computations.

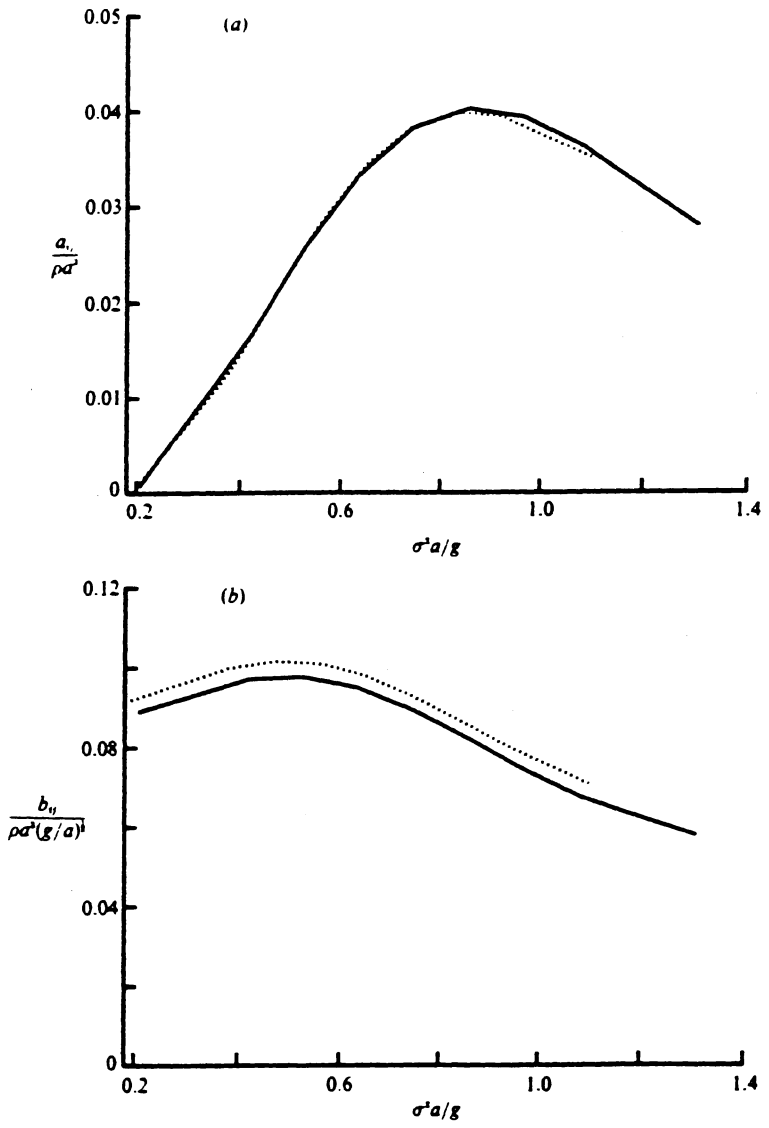

Figure 5: (a) (Total) added mass a_{13} (solid line) and $-a_{31}$ (dotted line) and (b) (total) damping b_{13} (solid line) and $-b_{31}$ (dotted line) for small translatory speed $U/\sqrt{ga} = 0.04$. $a_{ij} + b_{ij}/i\sigma = f_{ij}$. Half-immersed sphere with radius a. Same discretization as in figure 2. $h = \infty$.

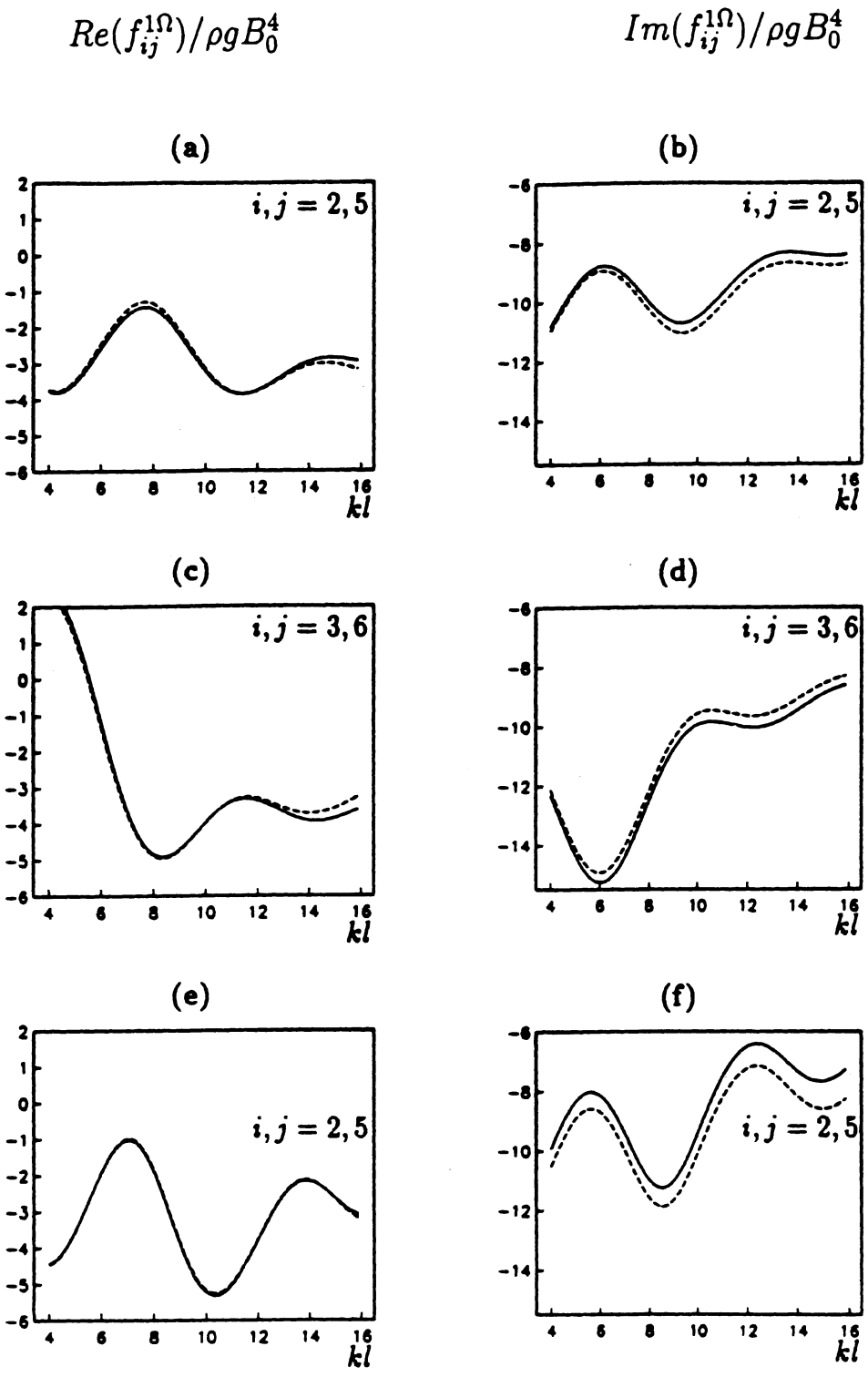

Figure 6: Added mass $Re(f_{ij}^{1\Omega})$ and damping $Im(f_{ij}^{1\Omega})$. (a)–(d) ship 1. Same discretization as in figure 2. (e)–(f) TPS (760 panels on S_B, 900 panels on S_F). Solid line: $f_{ij}^{1\Omega}$. Dashed line: $-f_{ji}^{1\Omega}$. $h = \infty$.

6 The body responses

The body responses are found from the equation of motion, where the usual hydrostatic forces are accounted for in addition to the added mass, damping and exciting forces. Accounting for the slow translatory modes we obtain rather simple extensions of the equation of motion at zero speed. When we allow the body to perform a slow rotation, we must also account for the non-Newtonian Coriolis force. We then find that the equation of motion for $\xi_j^{1\Omega}$ reads (note that we may use ω instead of σ since there is no coupling between U, V and Ω to leading order)

$$(-\omega^2(M_{ij}+f_{ij}^0)+c_{ij})\xi_j^{1\Omega} = A(X_i^{1\Omega}+iX_{i\beta}^0)+\omega^2[(f_{ij}^{1\Omega}-2iM_{ij}^c)\xi_j^0+2i(M_{ij}+(Kf_{ij}^0)_{,K})\xi_{j\beta}^0], \quad (78)$$

see derivation in reference 13. Here, M_{ij} is the usual body matrix, and the term involving M_{ij}^c is due to the Coriolis force. M_{ij}^c is determined by

$$M_{ij}^c = \begin{pmatrix} 0 & -M & 0 & MZ_G & 0 & -MX_G \\ M & 0 & 0 & 0 & MZ_G & -MY_G \\ 0 & 0 & 0 & 0 & 0 & 0 \\ -MZ_G & 0 & 0 & 0 & -I_{xy} & D_{yz} \\ 0 & -MZ_G & 0 & I_{xy} & 0 & -D_{xz} \\ MX_G & MY_G & 0 & -D_{yz} & D_{xz} & 0 \end{pmatrix} \quad (79)$$

where M denotes the mass of the body, (X_G, Y_G, Z_G) the center of gravity, and

$$I_{xy} = \int_M z^2 dM, \quad D_{xz} = \int_M xz dM, \quad D_{yz} = \int_M yz dM. \quad (80)$$

We note that M_{ij}^c is antisymmetric and corresponds to a rotation of the velocity vector about the vertical axis, an expected result due to the form of the Coriolis force.

6.1 The frequency of oscillation of mode number j

While the frequency of encounter determines the frequency of oscillation of a body (ship) with translatory motion in waves, the frequency of oscillation of a rotating ship is not so straightforward to determine, at first glance. For example, with the exceptions of head waves and following waves, the encounter frequency of the incoming waves observed at the bow and the aft of a rotating ship is different, and one expects the frequency of oscillation of the different modes of motion to occur at some frequency in-between these two extremes. Turning to mathematical formulae we have for the incoming waves in the frame of reference of the ship

$$\Phi^I = Re[(Aig/\omega)\phi^I e^{i\sigma t - ikR\cos(\beta-\theta)}], \quad z = 0. \quad (81)$$

The phase of the motion is then determined by

$$\sigma t - kR\cos(\beta-\theta). \quad (82)$$

From this we find the frequency of oscillation by

$$
\begin{aligned}
&\frac{d}{dt}(\sigma t - kR\cos(\beta-\theta)) \\
&= \sigma + kR\sin(\beta-\theta)\frac{d\beta}{dt} \\
&= \sigma - \Omega kR\sin\beta\cos\theta + \Omega kR\cos\beta\sin\theta \\
&= \sigma - \Omega kx\sin\beta + \Omega ky\cos\beta
\end{aligned} \tag{83}
$$

where we have used that $d\beta/dt = -\Omega$. Thus, the frequency of the waves observed at the bow of the ship is $(x = l/2, y = 0)$

$$\sigma - \Omega kl\sin\beta/2 \tag{84}$$

while at the aft $(x = -l/2, y = 0)$

$$\sigma + \Omega kl\sin\beta/2. \tag{85}$$

Now, the frequency of the oscillatory motions of the body may be determined in a similar way. For the motion in mode number j we have

$$\xi_j e^{i\sigma t} = |\xi_j| e^{i\sigma t + i\delta_j}. \tag{86}$$

The phase of the motion is then determined by

$$\sigma t + \delta_j \tag{87}$$

giving for the local frequency

$$\frac{d}{dt}(\sigma t + \delta_j) = \sigma - \Omega\frac{\partial\delta_j}{\partial\beta}. \tag{88}$$

The phase angle δ_j is found by first taking the logaritm of (86), i.e.

$$\ln\xi_j + i\sigma t = \ln|\xi_j| + i\sigma t + i\delta_j, \tag{89}$$

and then taking the imaginary part, i.e.

$$\delta_j = Im(\ln\xi_j) \tag{90}$$

giving

$$\frac{\partial\delta_j}{\partial\beta} = Im\Big(\frac{1}{\xi_j}\frac{\partial\xi_j}{\partial\beta}\Big). \tag{91}$$

Provided that $|\xi_j^0| >> |\tau(\Omega)\xi_j^{1\Omega}|$ we may replace ξ_j by ξ_j^0 in (91), i.e.

$$\frac{\partial\delta_j}{\partial\beta} \simeq \frac{\partial\delta_j^0}{\partial\beta} = Im\Big(\frac{1}{\xi_j^0}\frac{\partial\xi_j^0}{\partial\beta}\Big). \tag{92}$$

Thus, the frequency of mode number j of the ship reads

$$\tilde{\sigma} = \omega - kU\cos\beta - kV\sin\beta - \Omega Im\Big(\frac{1}{\xi_j^0}\frac{\partial \xi_j^0}{\partial \beta}\Big). \tag{93}$$

Likewise, we may deduce that the frequency of the exciting force becomes

$$\tilde{\sigma} = \omega - kU\cos\beta - kV\sin\beta - \Omega Im\Big(\frac{1}{X_j^0}\frac{\partial X_j^0}{\partial \beta}\Big). \tag{94}$$

We show in figures 7 – 8 some examples of the responses in the vertical modes of motion of ship 1 and the TPS in slow rotation. The figures show that $\xi_{3,5}^{1\Omega}$ are much larger than the counterparts at $\Omega = 0$. Furthermore, both figures show that the frequency of the rotating ship becomes different in the heave and pitch modes of motion. For ship 1 we note that the frequency of the response and the exciting force is the same in the respective modes, while for the TPS the exciting force X_3 and the response ξ_3 have different frequencies, as shown in figure 7c. For this ship the frequency in pitch becomes large for kl close to 13.5. This is, however is of no concern, since the amplitude $|\xi_5|$ is very small close to this wavenumber.

In figure 9 we show the properties of the surge motion due to a rotating ship 1 for fixed wavenumber and wave heading varying between 0° and 180°. Of interest, among others, is to see how the frequency of oscillation behaves for wave heading close to 90° (beam seas), where the surge motion disappears. We observe that δ_1^0 jumps at this wave heading, but this does not affect the derivative of δ_1^0 with respect to the wave angle, when we approach 90° from above or below. Even $\partial\delta_1^0/\partial\beta = Im\Big((\partial\xi_1^0/\partial\beta)/\xi_1^0\Big)$ is smooth and becomes zero for $\beta \to 90°$, in spite of that ξ_1^0 becomes zero there.

7 Concluding remarks

In this first report of the project entitled "The complete wave drift damping and applications" we have described the linear part of a method for obtaining the complete wave drift damping matrix. This includes the basic equations and perturbation expansions, formulation of boundary value problems for a set of potentials and the corresponding integral equations, the linear pressure and surface elevation, the linear forces and motions. The theory is illustrated by several exmples. In the next parts of the project we focus first on the second order quantities like force, moment and energy balance, and thereafter on case studies where the complete theory is applied. These parts of the project will be documented by similar reports as this one.

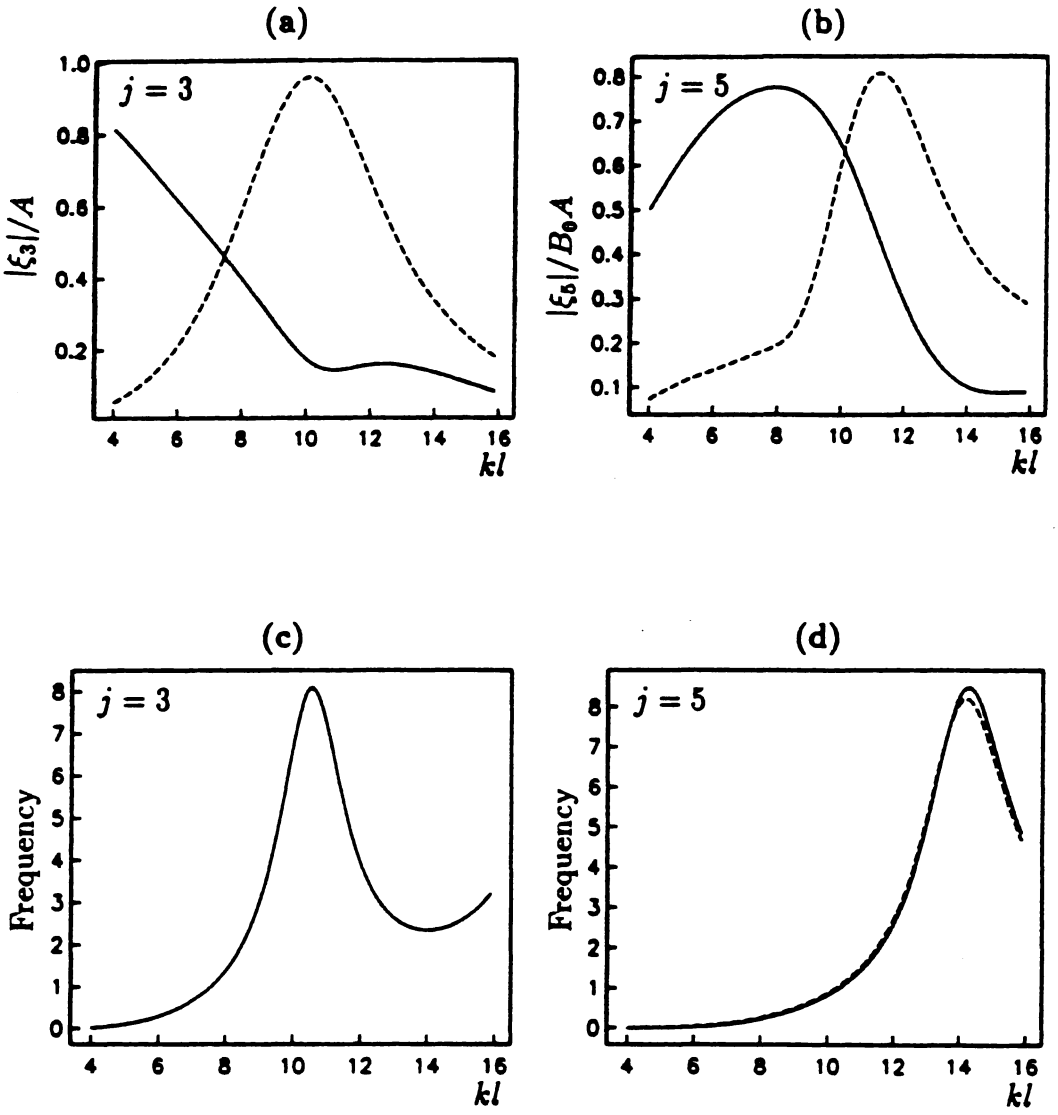

Figure 7: (a) and (b): Vertical responses of ship 1. Solid line: $|\xi_3^{1\Omega}| \times 10^{-1}$, $|\xi_5^{1\Omega}| \times 10^{-1}$. Dashed line: $|\xi_3^0|$, $|\xi_5^0|$. (c) Coefficient of relative decrease/increase in frequency due to rotation for the heave mode and (d) the pitch mode. Solid line: $Im[(\partial\xi_j^0/\partial\beta)/\xi_j^0]$ (motion), Dashed line: $Im[(\partial X_j^0/\partial\beta)/X_j^0]$ (exciting force). $\beta = 135°$. $h = \infty$. Same discretization as in figure 3.

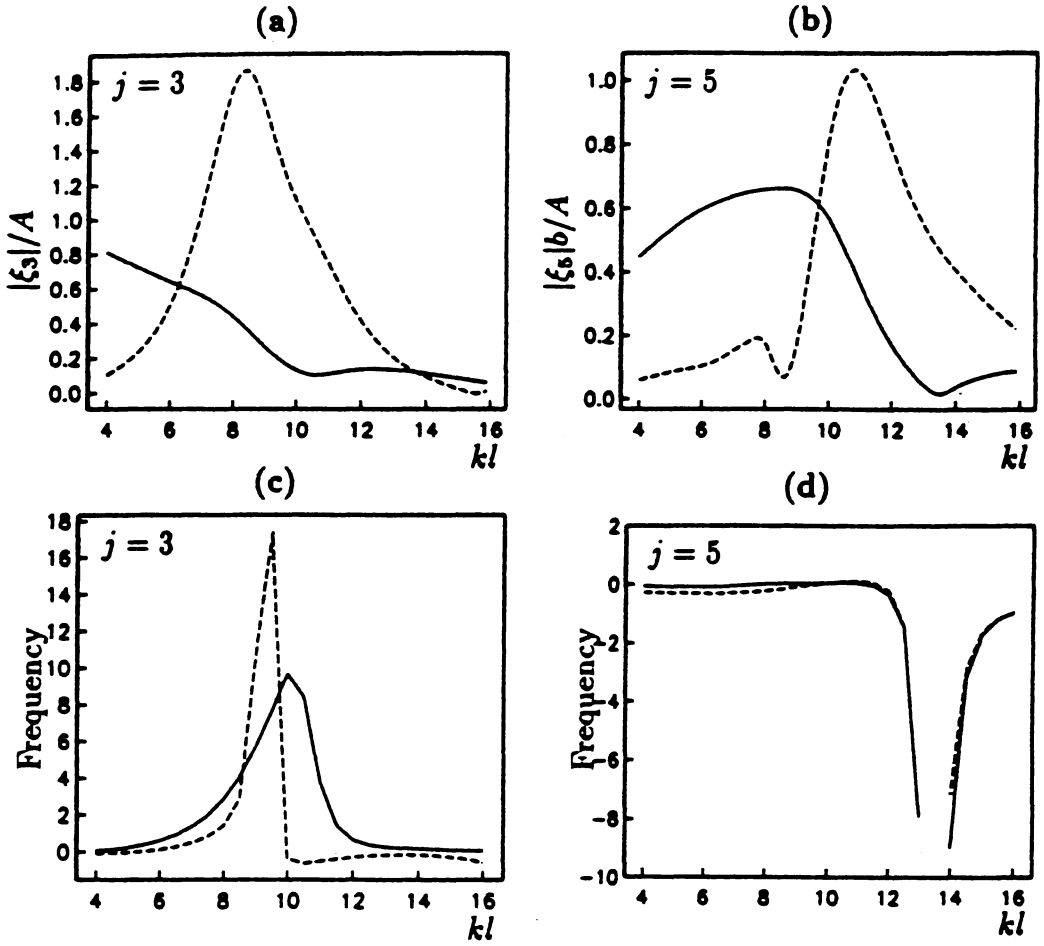

Figure 8: Same as figure 7, but for TPS.

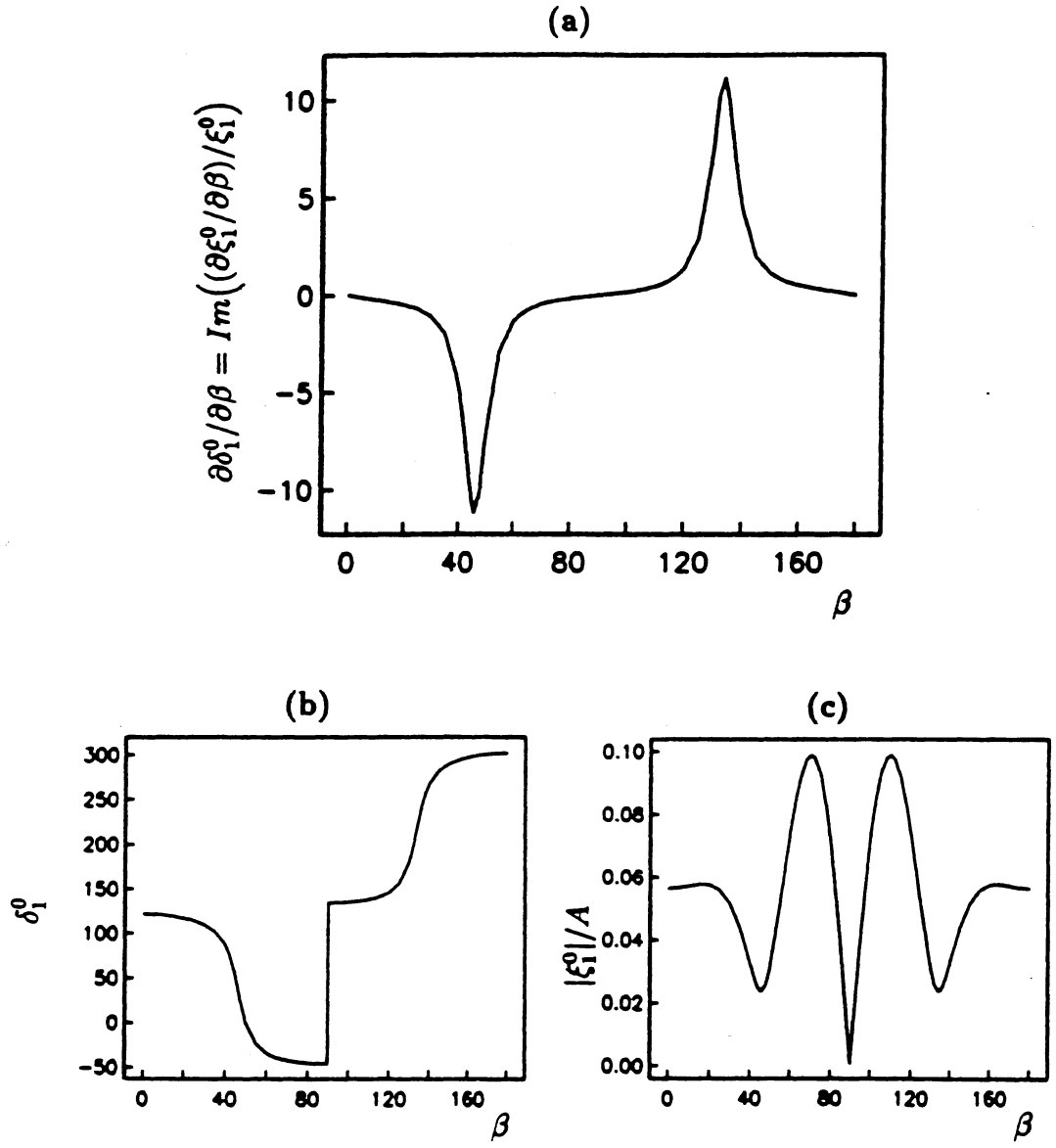

Figure 9: Surge motion of ship 1 as function of the wave angle β. (a) Coefficient of relative decrease/increase in frequency, $Im[(\partial\xi_1^0/\partial\beta)/\xi_1^0]$, due to the rotation, (b) The phase angle δ_1^0 and (c) $|\xi_1^0|$.

8 List of symbols

The list is ordered chronologically in accordance with the contents of the report.

$O - xyz$ – coordinate system in relative frame of reference
$\mathbf{i}, \mathbf{j}, \mathbf{k}$ – corresponding unit vectors
$U\mathbf{i} + V\mathbf{j} + \Omega\mathbf{k}$ – slow velocities of the body, Ω: rotation about the vertical axis
Φ^I, ϕ^I – incoming wave potential, see eq. 1
A – amplitude of incoming waves
ω – frequency of incoming waves in the fixed frame of reference
k – wavenumber of incoming waves
β_0 – wave angle in fixed frame of reference
β – wave angle (between x-axis and wave direction) in relative frame of reference
g – acceleration of gravity (=9.81m/s)
$K = \omega^2/g$
h – water depth
$i = \sqrt{-1}$
$\sigma = \omega - Uk\cos\beta - Vk\sin\beta$ – encounter frequency
R and θ – defined by $x = R\cos\theta$, $y = R\sin\theta$
α – rotation angle of the body in the fixed frame of reference
l – characteristic length of the body, ship length
$\tau(U) = U\omega/g$
$\tau(V) = V\omega/g$
$\tau(\Omega) = \Omega/\omega$
$\mathbf{v}$ – fluid velocity in the relative frame of reference
$\mathbf{v}'$ – fluid velocity in the fixed frame of reference
Φ' – velocity potential, $\nabla\Phi' = \mathbf{v}'$
Φ – linear wave potential, proportional to A
χ^U – potential due to slow motion in x-direction (without waves)
χ^V – potential due to slow motion in y-direction (without waves)
χ^Ω – potential due to slow rotation about the vertical axis (without waves)
$\psi^{(2)}$ – time-averaged potential proportional to A^2
$\mathbf{w}^U = -\mathbf{i} + \nabla\chi^U$
$\mathbf{w}^V = -\mathbf{j} + \nabla\chi^V$
$\mathbf{w}^\Omega = -\mathbf{k} \times \boldsymbol{x} + \nabla\chi^\Omega$
$\mathbf{w} = U\mathbf{w}^U + V\mathbf{w}^V + \Omega\mathbf{w}^\Omega$
Φ_t, Φ_{tt} – partial first and second derivatives of Φ with respect to time
Φ_z – partial derivative of Φ with respect to z
ϕ^0_{jK} – partial derivative of ϕ^0_j with respect to K
∇_h – horizontal gradient
ϕ_D – diffraction potential
$\phi_D = \phi^0_D + \tau(U)\phi^{1U}_D + \tau(V)\phi^{1V}_D + \tau(\Omega)\phi^{1\Omega}_D$ – perturbation expansion of ϕ_D

ϕ_j – radiation potential
ϕ_j^0, ϕ_j^{1U}, ϕ_j^{1V}, $\psi_j^{1\Omega}$ $\phi_j^{11\Omega}$ – perturbation potentials due to ϕ_j
ξ_j – response amplitude in mode number j ($j = 1, ..., 6$)
ξ_j^0, ξ_j^{1U}, ξ_j^{1V}, $\xi_j^{1\Omega}$ – perturbations of ξ_j
$\mathbf{n} = (n_1, n_2, n_3)$ – unit normal vector of the body
$\boldsymbol{x} \times \mathbf{n} = (n_4, n_5, n_6)$
δ_{ij} – Kroenecker delta
$H_j^0(\theta)$ – far-field amplitude of ϕ_j^0
$L_h(\phi, \chi) = 2\nabla_h\phi \cdot \nabla_h\chi + \phi\nabla_h^2\chi$ – operator at $z = 0$, enters in free surface condition
m_j^s – m-terms, $j = 1, ..., 6$, $s = U, V, \Omega$
H_j^U – far-field amplitude of $\phi_j^0 - \phi^I + \tau(U)\phi_j^{1U}$
H_j^V – far-field amplitude of $\phi_j^0 - \phi^I + \tau(U)\phi_j^{1V}$
k^{1U} – wavenumber, see eq. 41
k^{1V} – wavenumber, see eq. 42
$C_g(kh) = \tanh kh + kh/\cosh^2(kh)$ – see eq. 43
$\phi_j^{13\Omega}$ – part of $\phi_D^{1\Omega}$, $\psi_j^{1\Omega}$, see eq. 44
$H_j^{13\Omega}$ – far-field amplitude of $\phi_j^{13\Omega}$
G^0 – zero speed Green function
G^{1U}, G^{1V}, $G^{1\Omega}$ – auxillary functions, see eqs. 58 – 60
$\boldsymbol{\xi}' = (\xi', \eta', \zeta')$ – source point
S_B – wetted body surface
S_F – free surface
p – pressure
ρ – density of the fluid
ζ – elevation of free surface
F_j – force, see §4
X_j, X_j^0, X_j^{1U}, X_j^{1V}, $X_j^{1\Omega}$ – exciting forces, see §5
h^0 – far-field amplitude of G^0, see eq. 72
$\psi_j^{1U} = \phi_j^{1U} + 2k\cos\beta\phi_{jK}^0$ – potential
$\psi_j^{1V} = \phi_j^{1V} + 2k\sin\beta\phi_{jK}^0$ – potential
$B(x)$ – local beam of ship 1
B_0 – beam of ship 1 and TPS
l – ship length
$f_{jk} = a_{jk} + b_{jk}/i\sigma$ – added mass (real part) and damping (imaginary part)
f_{jk}^0, f_{jk}^{1U}, f_{jk}^{1V}, $f_{jk}^{1\Omega}$ – perturbations of f_{jk}
M – body mass
M_{ij} – body mass matrix
M_{ij}^c – matrix accounting for the Coriolis force, see §6
$\tilde{\sigma}$ – local frequency
δ_j, δ_j^0 – phase angles of responses

References

1) J. Grue & E. Palm (1985). Wave radiation and wave diffraction from a submerged body in a uniform current. J. Fluid Mech. 151.

2) J. Grue & E. Palm (1986). The influence of a uniform current on slowly varying forces and displacements. Appl. Ocean Res. 8.

3) J. Nossen, J. Grue & E. Palm (1991). Wave forces on three-dimensional floating bodies with small forward speed. J. Fluid Mech. 227.

4) J. Grue & E. Palm (1991). Currents and wave forces on ships and marine structures. In: Dynamics of marine vehicles and structures in waves, edited by W. G. Price, P. Temarel and A. J. Keane. Invited paper for the IUTAM symposium, Brunel University, Uxbridge, U.K. 1990.

5) J. Grue & E. Palm (1991). Wave loading on ships and platforms at a small forward speed. In: Proc. 10th Int. Conf. on Offshore Mech. and Arctic Engng. (OMAE), Eds. S. K. Chakrabarti et al.

6) J. Grue (1992). Drift force and drift moment on ships advancing with a small speed in oblique waves. Ship Tech. Res. 39.

7) Grue, J. & Palm, E. (1992). The mean yaw moment on floating bodies advancing with a forward speed in waves. Proc. 16th Int. Conf. on Offshore Structures (BOSS'92), London, Great Britain. Eds. M. H. Patel and R. Gibbins.

8) J. Grue & E. Palm (1993). The mean drift force and yaw moment on marine structures in waves and current. J. Fluid Mech. 250.

9) J. Grue & D. Biberg (1993). Wave forces on marine structures with small speed in water of restricted depth. Appl. Ocean Res. 15.

10) J. Grue & E. Palm (1994). A boundary element method for predicting wave forces on marine bodies with slow yaw-motion. Proc. 7th Int. Conf. Behaviour of Offshore Structures (BOSS '94), MIT, ed. C. Chryssostomidis, Vol. 2. Pergamon.

11) J. Grue (1996). Interaction between waves and slowly rotating floating bodies. In: Waves and Nonlinear Processes in Hydrodynamics. Edited by J. Grue, B. Gjevik and J. E. Weber. Kluwer Academic Publishers.

12) J. Grue & E. Palm (1996). Wave drift damping of floating bodies in slow yaw motion. J. Fluid Mech. 319.

13) S. Finne & J. Grue (1996). The complete radiation-diffraction problem for wave-drift damping in the yaw mode of motion. J. Fluid Mech. 357.

14) J. V. Wehausen and E. V. Laitone (1960). Surface waves. Handbuch der Physik IX.

15) J. Grue (1999). A note on the contributions to the wave-drift damping matrix from the time-averaged second order potential. Applied Ocean Res. 21.

II. THEORY. FORMULAE AND RESULTS FOR THE WAVE DRIFT DAMPING MATRIX

The complete wave drift damping matrix and applications

Part 2: Formulae and results for the wave drift damping matrix

by

John Grue and Styrk Finne

Mechanics Division,
Department of Mathematics,
University of Oslo, Norway

CONTENTS

1 Introduction

This report contains "The wave drift damping matrix and applications, part 2", and describes the theory for and the numerical evaluation of the wave drift damping matrix B_{ij}. We also compute the horizontal drift force (F_x, F_y) and the drift moment M_z about the vertical axis, i.e.

$$\begin{pmatrix} F_x \\ F_y \\ M_z \end{pmatrix} = \begin{pmatrix} F_{x0} \\ F_{y0} \\ M_{z0} \end{pmatrix} - \begin{pmatrix} B_{11} & B_{12} & B_{16} \\ B_{21} & B_{22} & B_{26} \\ B_{61} & B_{62} & B_{66} \end{pmatrix} \begin{pmatrix} \tau(U) \\ \tau(V) \\ \tau(\Omega) \end{pmatrix} \tag{1}$$

where, $(F_{x0}, F_{y0}, M_{z0}) = (F_x, F_y, M_z)$ for $U = V = \Omega = 0$, and

$$\tau(U) = U\omega/g, \qquad \tau(V) = V\omega/g, \qquad \tau(\Omega) = \Omega/\omega. \tag{2}$$

(U,V,Ω denote slow velocities along the x, y, z-directions, ω wave frequency and g acceleration due to gravity.) The report is organized as follows: Section 2 describes wave drift damping results and computations of force and moment at zero speed. Results illustrating convergence and various checks of the method are also described. In section 3 the potentials of the wave field are described, section 4 contains formulae for the complete wave drift damping matrix B_{ij}, and section 5 contains formulae for the energy check. While section 2 is descriptive, sections 3–5 are mathematical.

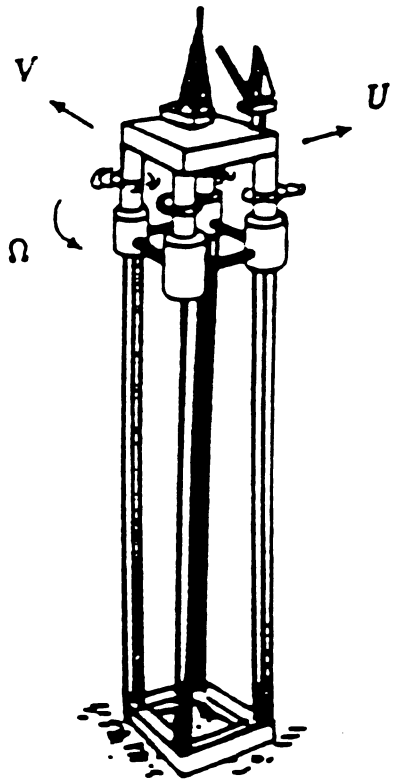

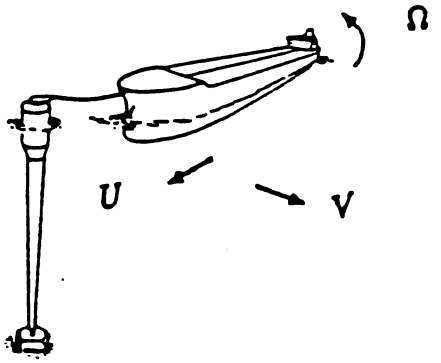

2 Wave drift damping results

2.1 Description of the main steps of theory and results

The mathematical problem is formulated in the relative frame of reference which follows the slow velocity of the floating body, and non-Newtonian forces (the Coriolis force) are accounted for. The first step is to compute the potentials which determine the components of the fluid flow at the geometry under consideration. This is obtained by solving the integral equations which are derived from a set of boundary value problems. The numerical solution is found by exploiting a low-order method which gives sufficient accuracy for practical purposes. We then evaluate the added mass and damping coefficients, the exciting forces and the linear motions of the body. In all parts of the formulation the slow drift motions of the body are accounted for, where the slow drift velocites U, V and Ω appear as prefactors like in (1)–(2). The linear part of the method is described in part 1 of this report, see reference [15].

In the next step we derive formulae for the wave drift damping matrix, with results given in section 4. We start with the equations of conservation of linear and angular momentum, where all terms are consistently accounted for. This means that terms proportional to the wave amplitude squared times the slow velocities in the three horizontal modes of motion are included. The formulae are relatively simple at the onset, but the final versions become rather complex. The physical and mathematical arguments used in the derivations are basically conservation of mass, various versions of Gauss', Stoke's and Green's theorems, in addition to some manipulations. The precise derivations are given in the references [3], [8], [9] for the formulae which determine B_{11}, B_{21}, B_{61}, B_{12}, B_{22}, B_{62} (translation). These coefficients are in this report developed on (novel) explicit form. The derivations for the angular mode, i.e. B_{16}, B_{26}, B_{66}, are given in the references [11], [12], [13]. The final formulae express the damping coefficients by:

i) contributions determined by the far-field amplitudes of the linear velocity potentials, where the effect of the slow drift velocities are taken into account;

ii) contributions determined by the far-field dipole moments of the potential governing steady velocities in the fluid, introduced by the linear wave field. These velocities couple to the slow drift velocities in the mathematical formulation (see reference [8]);

iii) and, for B_{66}, contributions due to linear body responses coupled by the matrix representing the effect of the Coriolis force and the restoring force matrix.

All the contributions i), ii), iii) are of importance and must generally be evaluated. For geometries with special motion characteristics, some of the terms may predominate, however. Computations for a ship (*Turret Production Ship*) indicate that the terms i) and ii) are of equal importance, a result which seems to be due to the relatively large body responses of this geometry. The contribution iii) may be somewhat smaller than the other terms. Preliminary computations of a *tension-leg platform* indicate that the terms of category i) give largest contribution. This is due to the particular geometry of a tension-leg platform and that such a platform has relatively small linear responses.

2.2 Wave drift damping computations

The wave drift damping coefficients are functions of the wave angle and the wavenumber, and extensive examples for the entire wave drift damping matrix is rather demanding. Here we will show some results which may illustrate the main trend for some of the damping coefficients. The results may serve as reference and basis for further computations. Several computations of six of the wave drift damping coefficients have been presented in the references [3]–[12], namely the damping coefficients B_{i1} and B_{i2}, $(i = 1, 2, 6)$, due to translation. We also show here novel computations for the damping coefficients in the yaw mode, i.e. B_{16}, B_{26} and B_{66}. We perform computations for two ship models and an offshore platform.

2.2.1 Ships

The first ship model has circular section and beam $B(x)$ given by

$$B(x) = B_0[1 - (2x/l)^4], \quad |x| < l/2, \tag{3}$$

where l denotes the ship length and $l/B_0 = 5.6$. We refer to this model as Ship 1. The other ship is a Turret Production Ship (TPS) with length to beam ratio equal to 5.6. Results for B_{11} and B_{61} are shown in figures 1–2 for two different water depths for the TPS and Ship 1 (to be precise, the geometry used to produce figure 2 is slightly different from (3)). The damping coefficients B_{16}, B_{26} and B_{66} are shown in figures 3–5 for various wavenumbers and wave headings, where the latter is defined as the angle between the length direction of the ship, towards the bow, and the wave direction. Wave angle 90° means beam seas, 135° quartering seas and 180° head seas. The wavenumber range is $4 < kl < 16$, which means that for a ship with length $230m$ the wave length $\lambda = 2\pi/k$ is in the range

$$90\text{m} < \lambda < 360\text{m} \tag{4}$$

The figures 3–5 show trends which mainly are:

- The values of B_{16} and B_{26} give forces comparable to B_{11} and B_{12} for angular velocity times ship length Ωl equal to translatory speed U.
- B_{16} and B_{26} may be both positive and negative. There are no physical reasons which contradict this.
- B_{16} and B_{26} are almost the same for the two ship models for waves with headings 157°, 180°. This is not true for quartering waves and beam seas, where both B_{16} and B_{26} are large but different for the ships. For $\beta = 90°$, $B_{26} = 0$ for Ship 1, due to symmetry.
- B_{66} is always positive for the ship models. This is not true for all geometries, however. Computations for an offshore platform show that B_{66} may be negative for some regions of the incoming wave length, see below.
- B_{66} becomes larger for the TPS than for Ship 1. This is most significant for beam seas. The effect on the damping coefficients due to the responses of the ship are found to be large. This result is obtained by comparing with computations in reference [12], where the effect of motions were discarded.

For comparison, we show in figures 6–8 computations of F_{x0}, F_{y0}, M_{z0}. A realistic ratio between Ω and ω may be 1:50, which means that the contribution from the damping matrix may significantly increase the total force or moment acting on the body by 20-50%.

2.2.2 Offshore platform

In the next examples the geometry is a model of an offshore platform, namely an array of four vertical circular cylinders with radius a, draught $3a$ and with the cylinder axes located at $(x, y) = (\pm 3.5a, \pm 3.5a)$. In this case the water depth is infinite. In figures 9–10 are presented results for the wave drift damping coefficient B_{11} and B_{66}. The results exhibit quite strong variations with respect to the wavenumber and the wave angle. In most cases the wave drift damping is positive. For some wavenumber and wave angle domains the wave drift damping becomes negative, however. This occurs for B_{11} when $0.5 < ka < 0.7$ ($\beta = 180°$). For B_{66} negative wave drift damping is most pronounced for $\beta = 45°$ and $0.6 < ka < 0.8$, $1.15 < ka < 1.35$. In figure 10 are also shown results by the method of Emmerhoff and Sclavounos who obtain the wave drift damping moment for vertical cylinders by pressure integration over the body (Sclavounos, personal communication). The agreement between the two different methods is good.

2.3 Convergence and the energy check

As mentioned in part 1 of this report [15] it is desirable to develop checks when deriving a rather complex method. This makes possible a verification of the theory and the numerical code. Another aspect is convergence of the method. These issues are illustrated in the examples in figures 11–14.

First is considered convergence of the added mass and damping coefficients f_{25} and $-f_{52}$, which should be equal, according to the theory. In figure 11 we show computations of these coefficients versus the inverse number of panels ($1/N$) on the wetted ship surface. The figure illustrates the accuracy of the computations, indicating that $f_{25} + f_{52} \to 0$ as $1/N \to 0$.

In figure 12 is studied convergence of B_{16} and B_{66} for Ship 1 for two different wave headings. The number of panels on the wetted body surface is N=392, 800, 1568, with corresponding number of panels on the free surface N_F=1568, 3200, 6272. The results document convergence.

Figure 13 shows the energy check for Ship 1, illustrating that the energy in the method is conserved. A correct energy check, which is non-trivial, also documents soundness of the method. Similar computations are performed for other geometries (results not shown), giving the same positive check of the method.

In the last illustration we let Ship 1 rotate about an axis of 100 ship lengths away from the ship. This means that the ship is almost performing a translation. We then compare results for B_{11}, B_{16}/ks, B_{66}/s^2k in incoming head waves, where $s = 100l$ and l the ship length, k the wavenumber. These coefficients, obtained by three completely different formulae, should be equal with this scaling, a result which is confirmed by the computations shown in figure 14, giving another check of the method.

$\sqrt{KL} \times \frac{B_{11}}{\rho g A^2 B^2}$

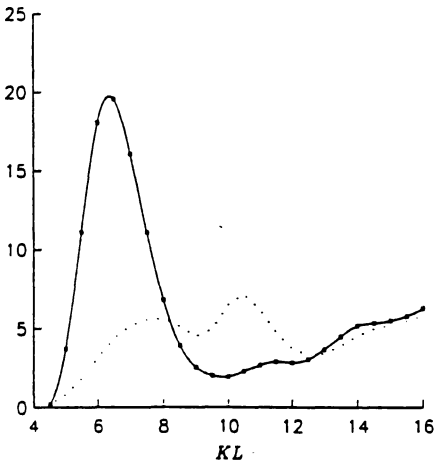

$\sqrt{KL} \times \frac{B_{11}}{\rho g A^2 B^2}$

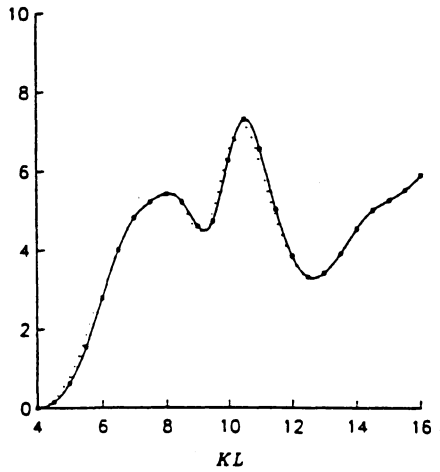

Figure 1: Damping coefficient B_{11}. 0° (following waves). (a) TPS, $h/T = 1.2$. (b) TPS, $h = \infty$. Examples from reference [9]. L denotes ship length, T draught, B beam.

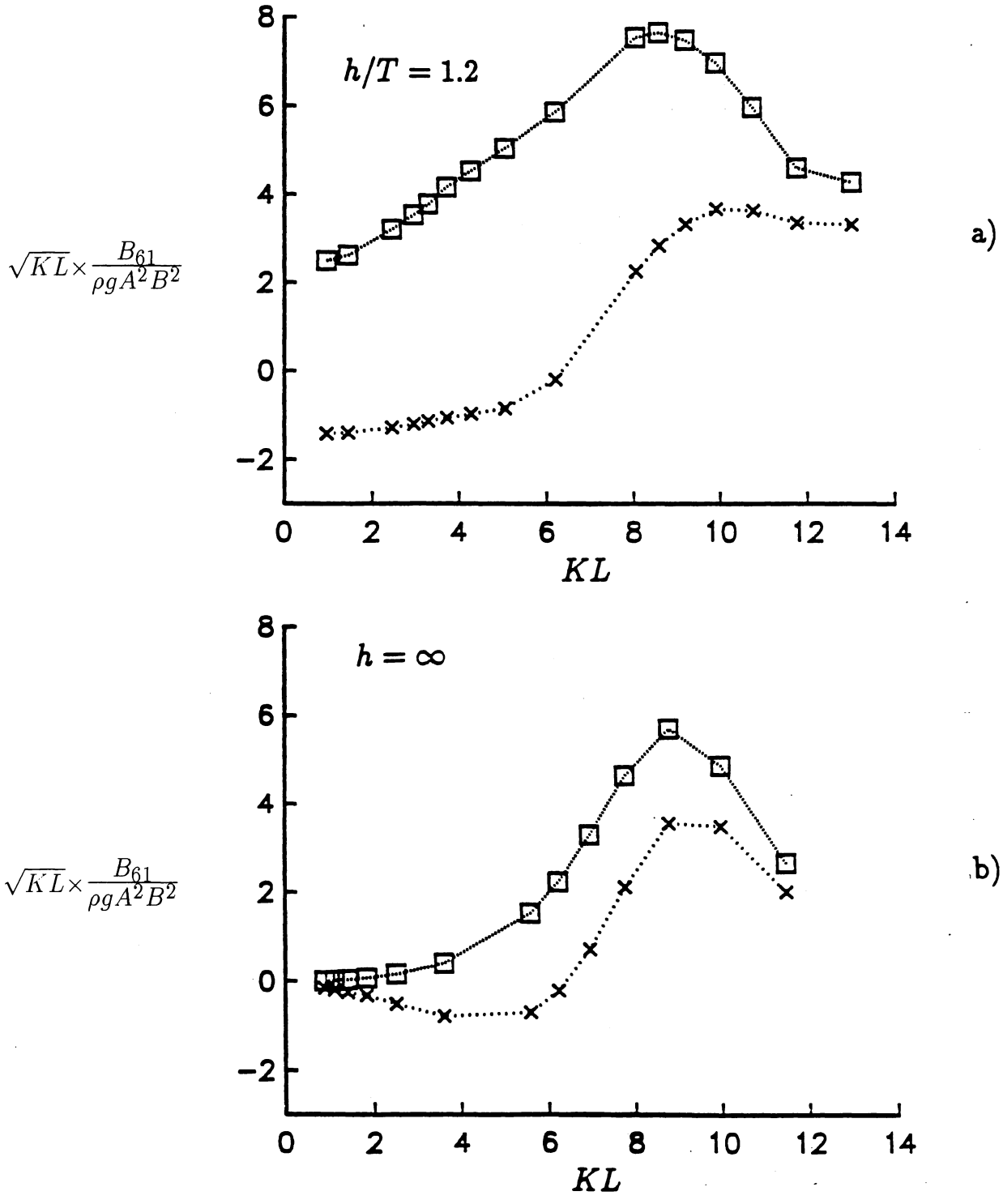

Figure 2: Damping coefficient B_{61}. 135° (quartering waves). (a) Ship1, $h/T = 1.2$. (b) Ship1, $h = \infty$. Examples from reference [14]. L denotes ship length, T draught, B beam.

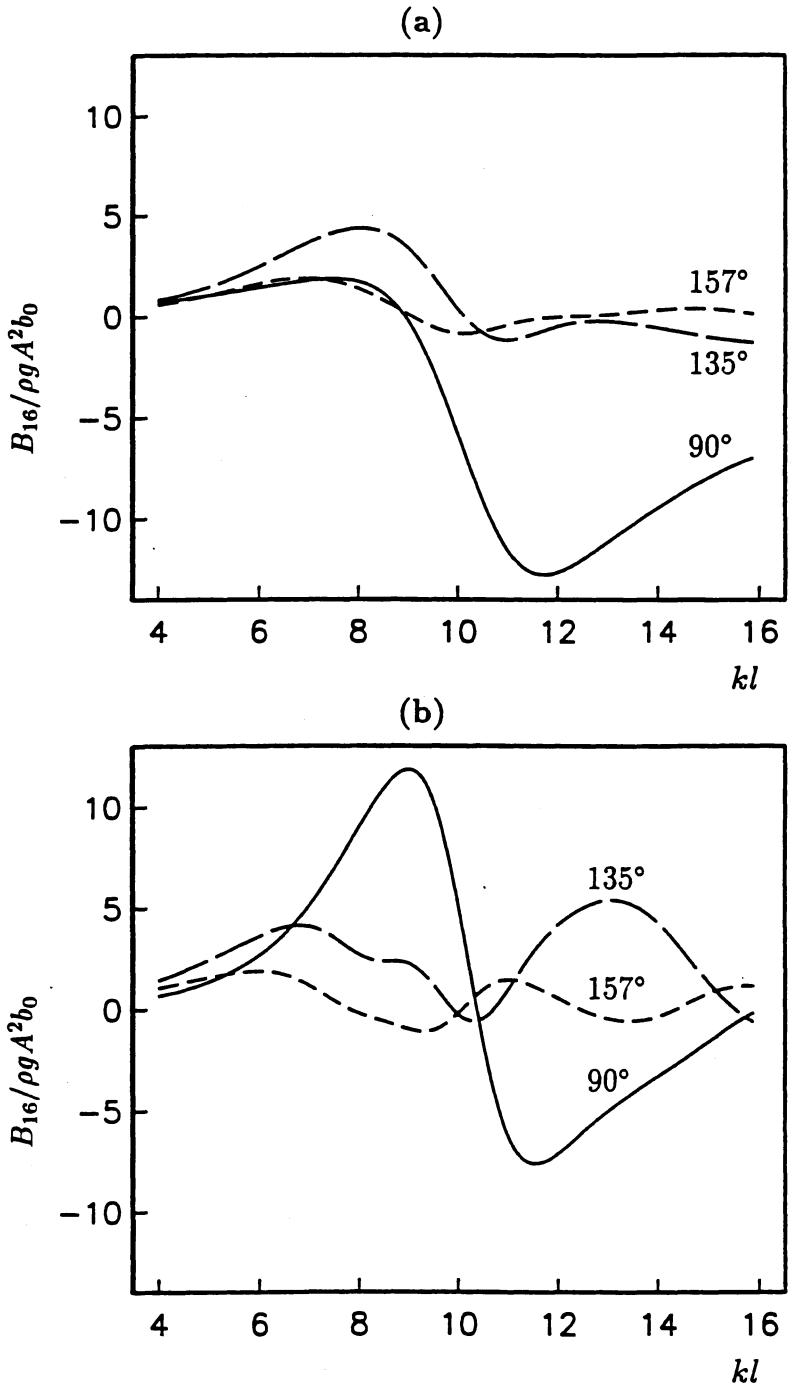

Figure 3: Damping coefficient B_{16} at different wave angles. 180° means head waves. (a) Ship1, 1568 panels on S_B. 6272 panels on S_F. (b) TPS, 760 panels on S_B. 1800 panels on S_F.

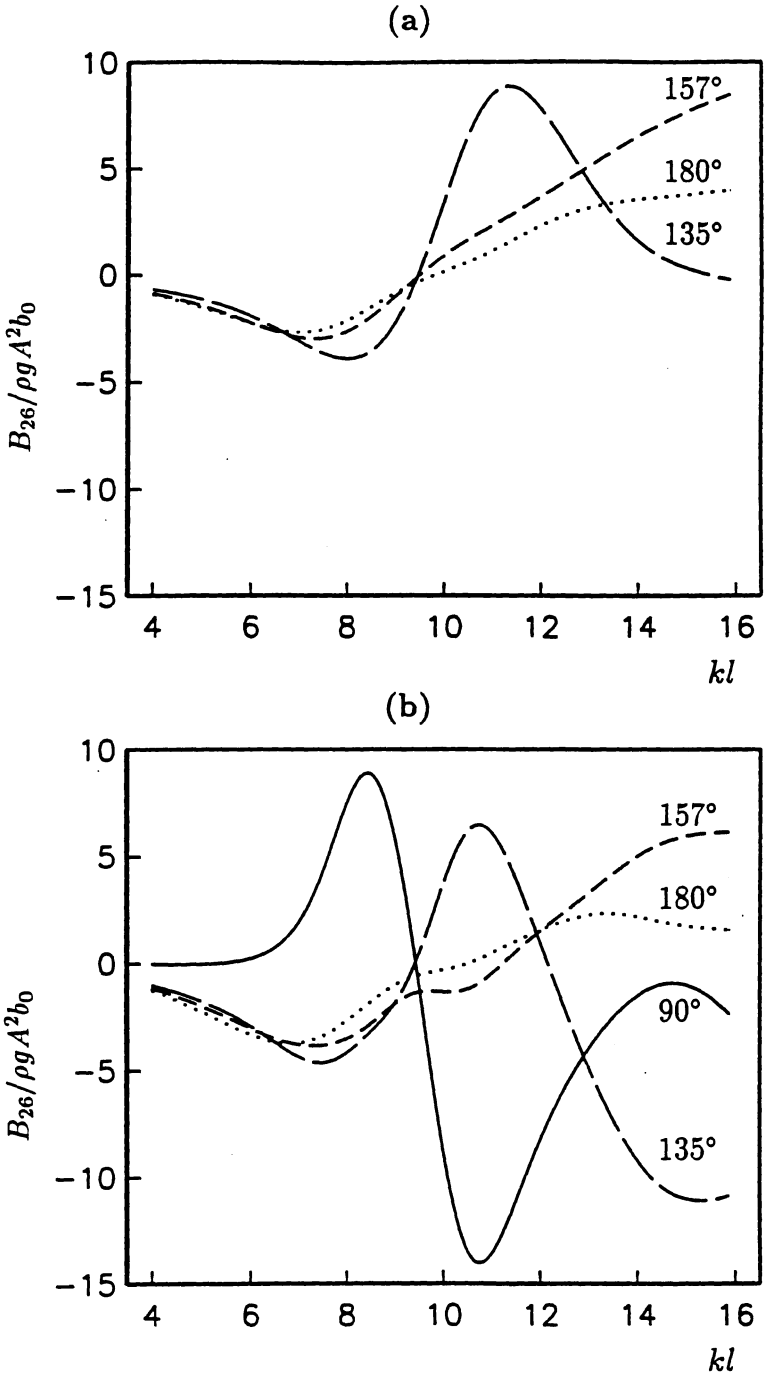

Figure 4: Same as figure 3, but B_{26}.

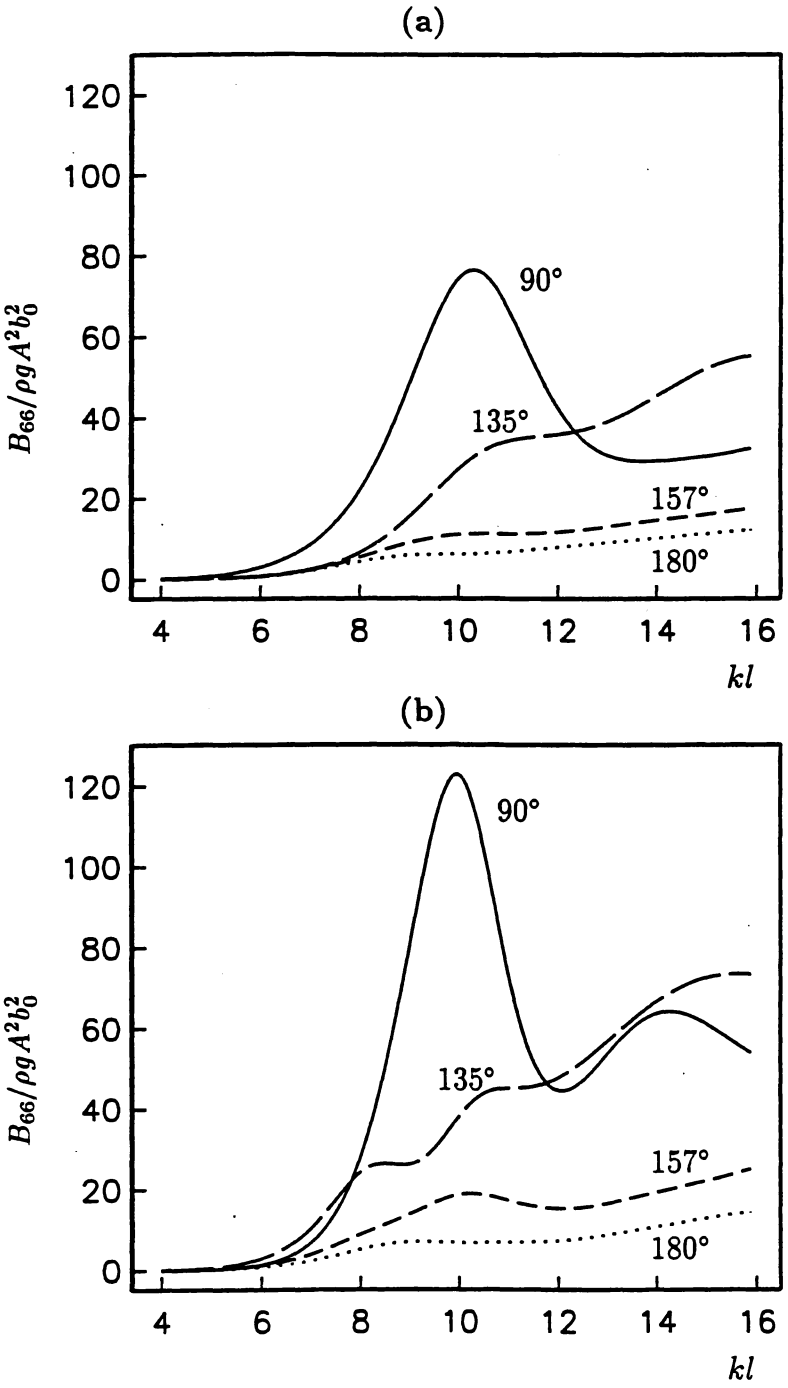

Figure 5: Same as figure 3, but B_{66}.

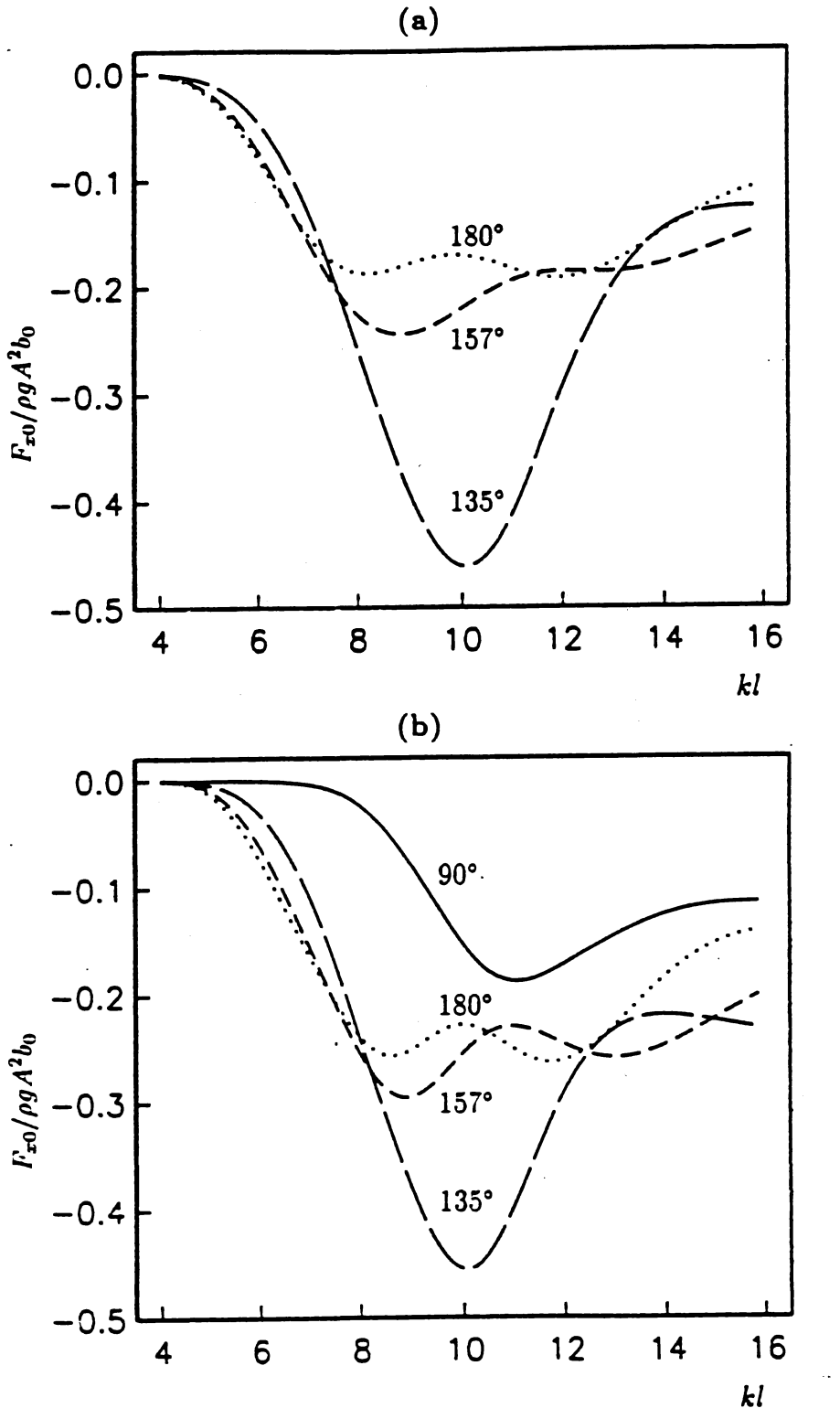

Figure 6: Drift force F_{x0} at different wave angles. (180° means head waves.) (a) Ship1, 1568 panels on S_B. 6272 panels on S_F. (b) TPS, 760 panels on S_B. 1800 panels on S_F.

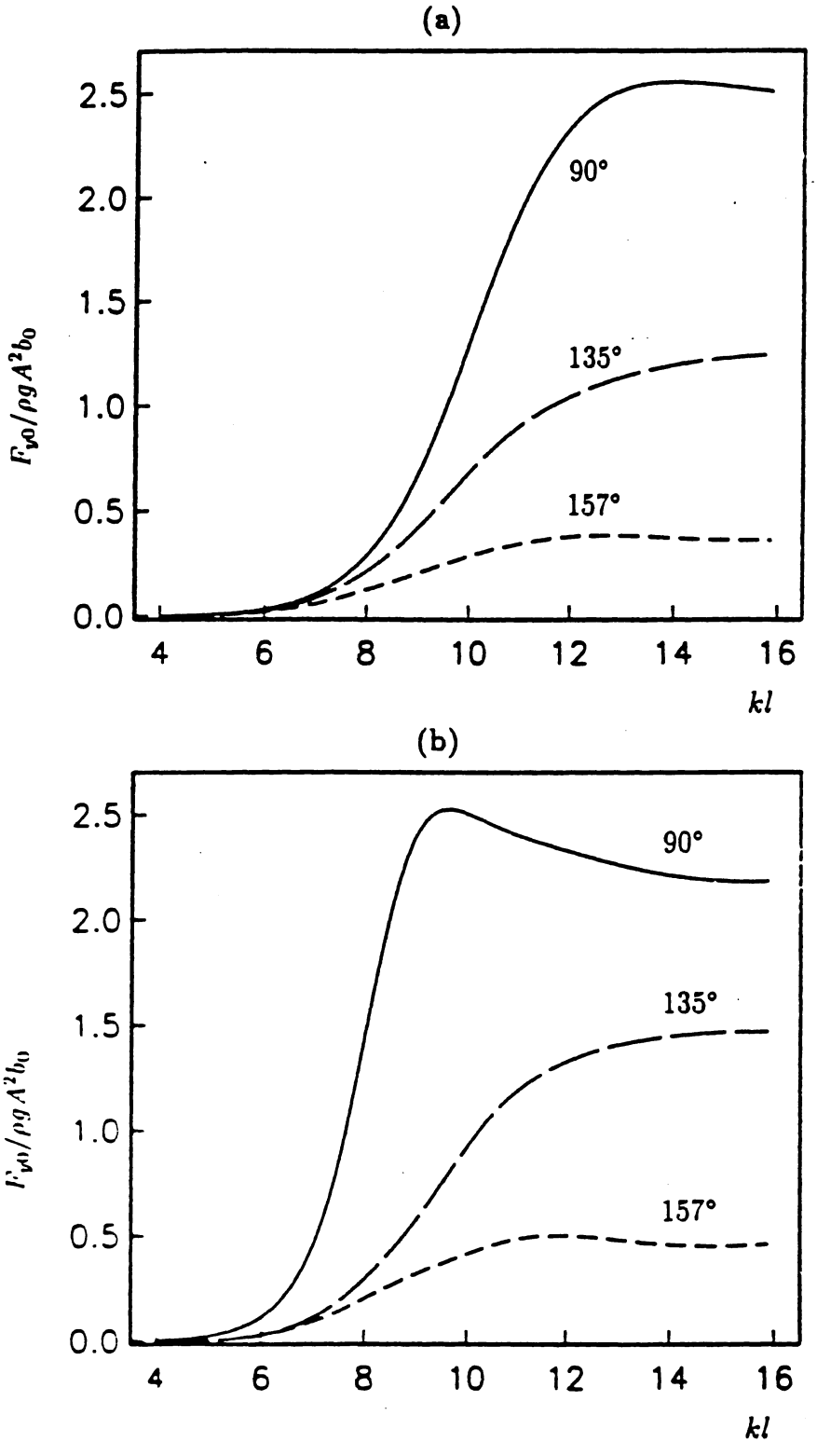

Figure 7: Same as figure 6, but F_{y0}

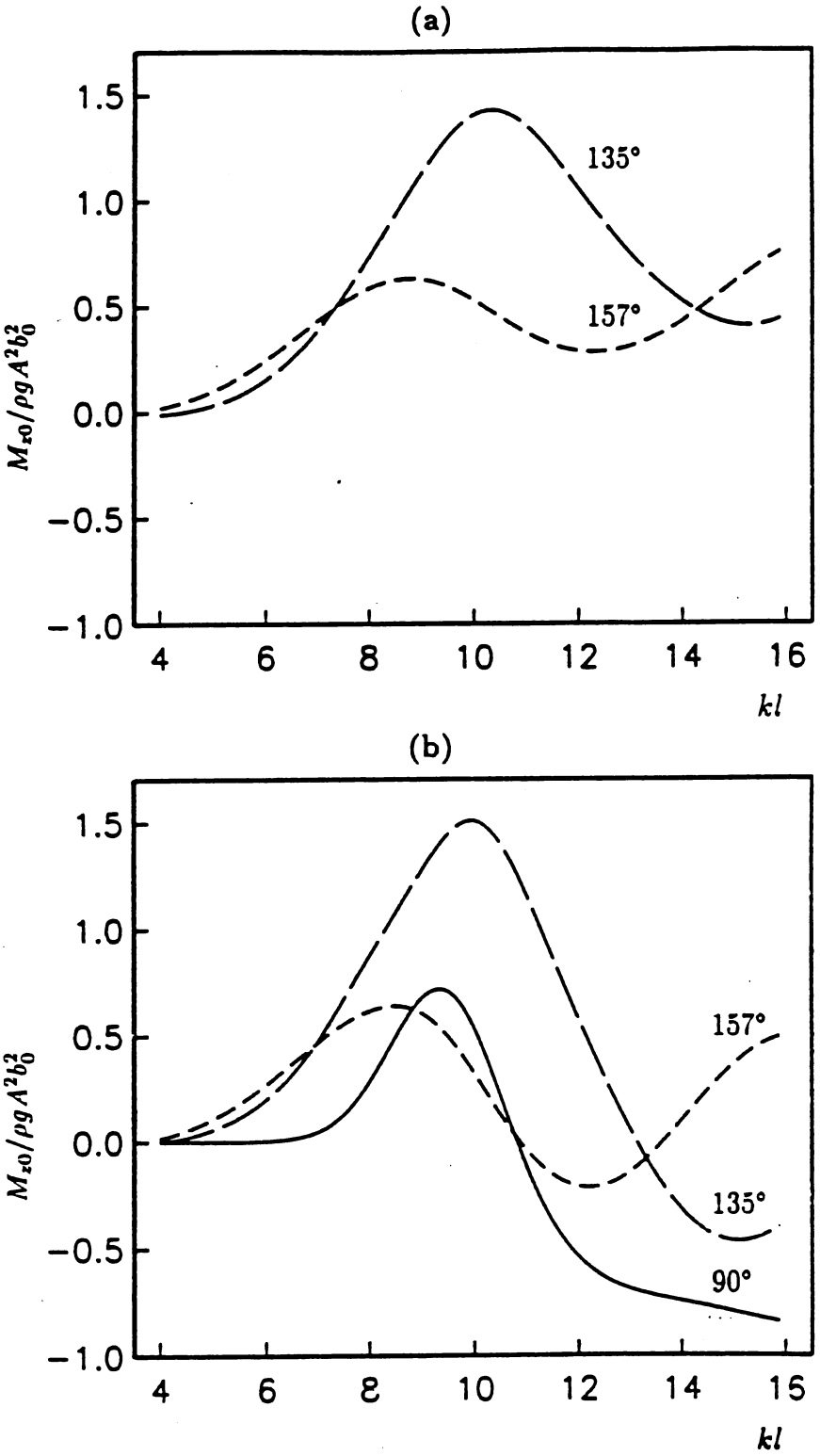

Figure 8: Same as figure 6, but M_{z0}

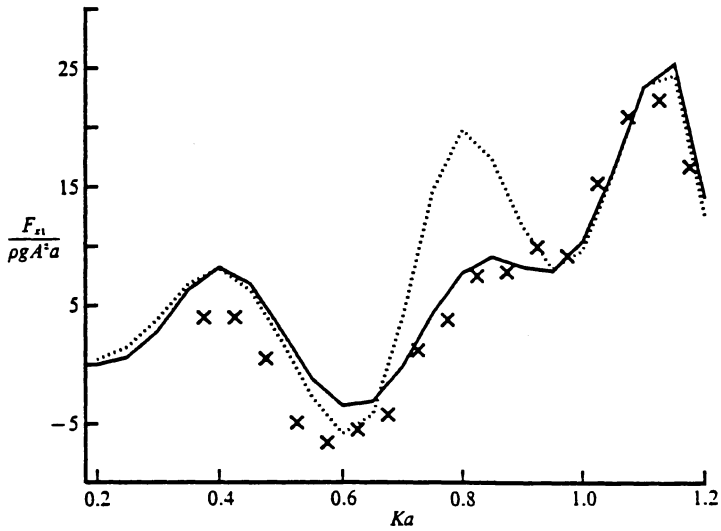

FIGURE 10. Wave drift damping coefficient for an offshore platform obtained by numerical differentiation of F_z at $Fr = \pm 0.005$. The platform is free to surge in head waves. Solid line. without pontoon; dotted line. with pontoon: ×. simplified method for the cylinder array.

Figure 9: Wave drift damping moment B_{11} for an array of vertical cylinders. Wave heading $\beta = 180°$. Example from Nossen, Grue and Palm [3], figure 10.

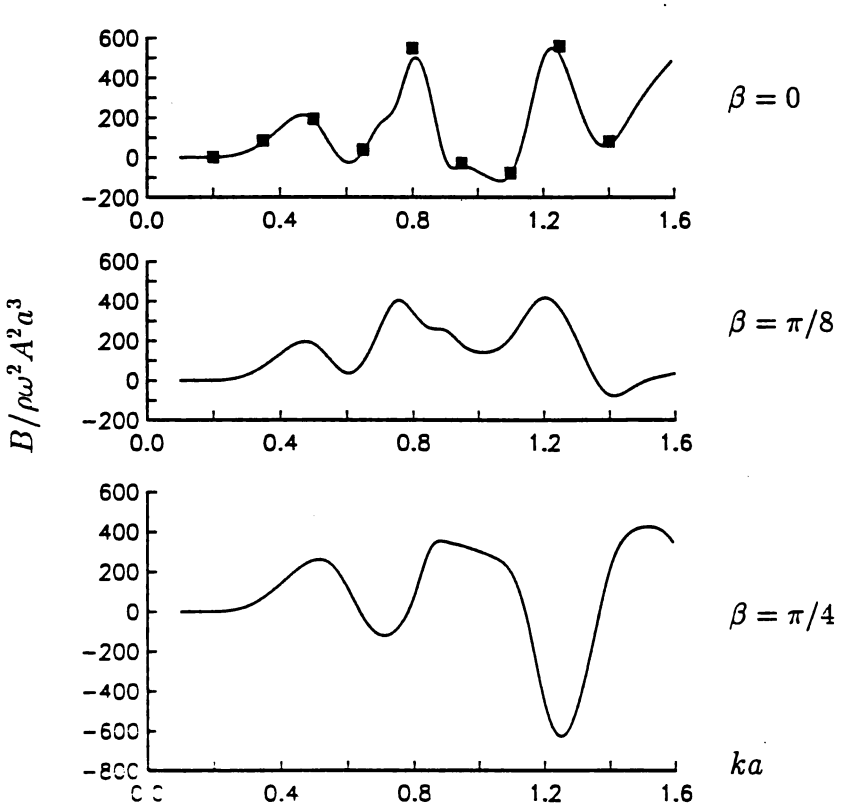

Figure 10: Wave drift damping moment B_{66} for an array of vertical cylinders. Three different wave headings: $\beta = 0$, $\beta = \pi/8$, $\beta = \pi/4$. $h = \infty$. Discretization: S_B: 784 panels. S_F: 936 panels. S_F discretized within a square with side $28a$. Black squares: The method of Emmerhoff and Sclavounos.

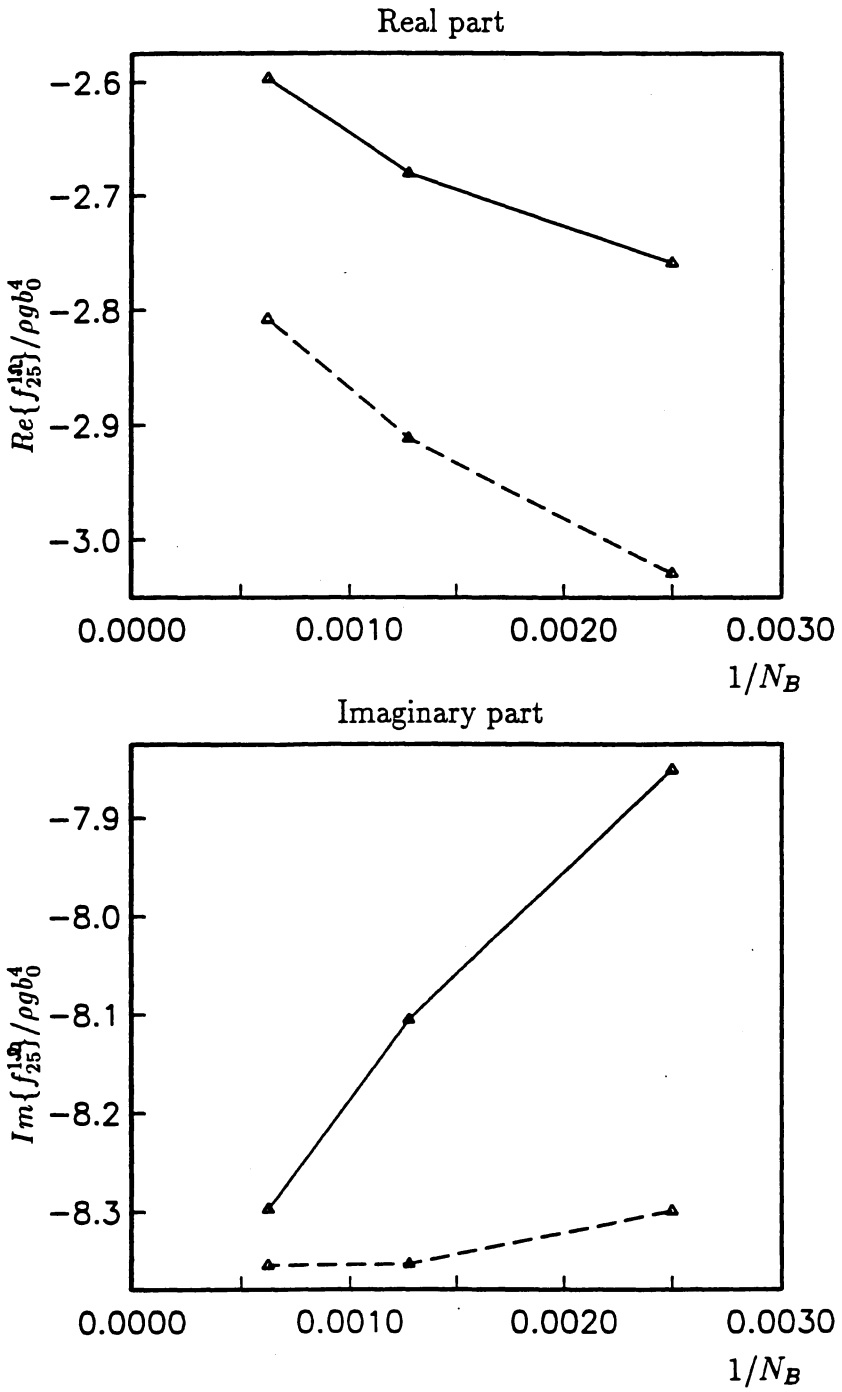

Figure 11: Convergence of $f_{25}^{1\Omega}$ (solid line) and $-f_{52}^{1\Omega}$ (dashed line) vs. N, the number of panels on S_B. Ship 1. $kl = 14.5$.

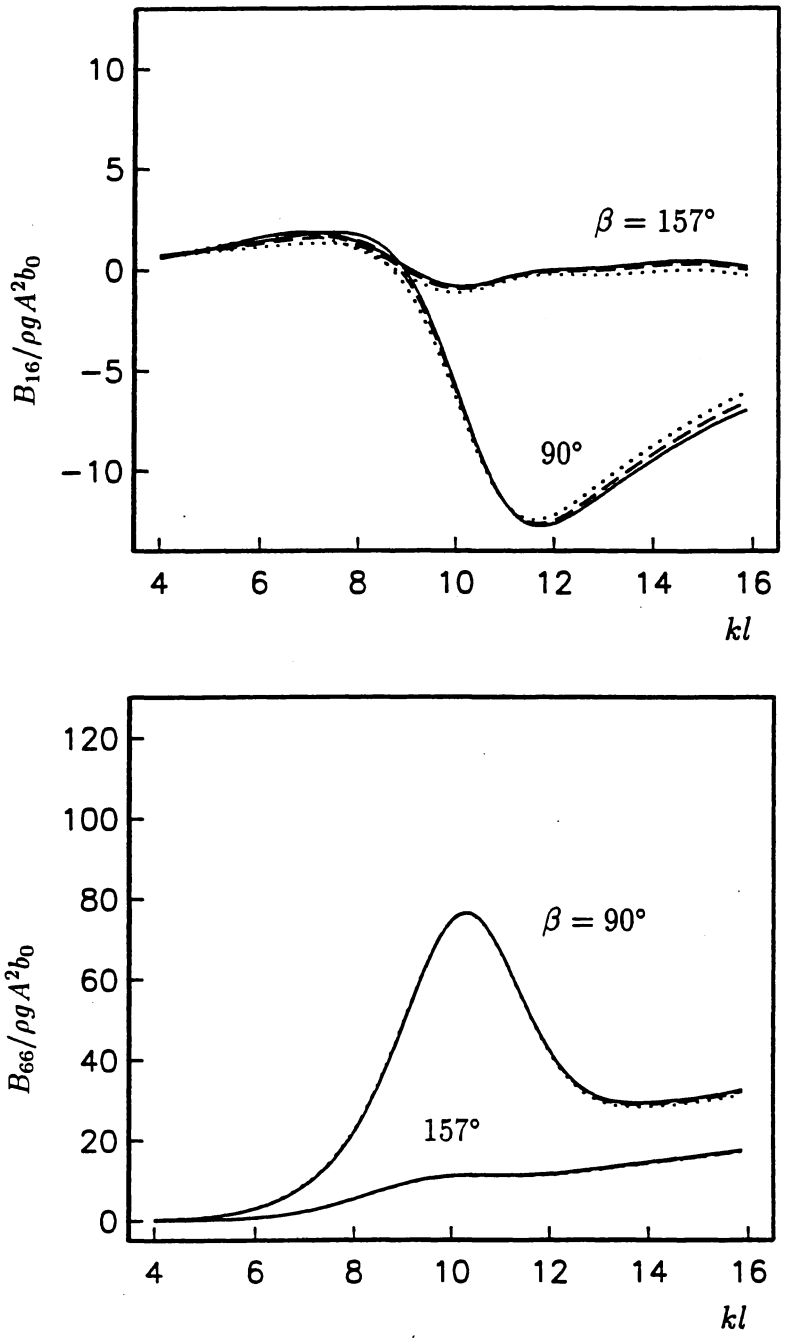

Figure 12: Convergence of B_{16} and B_{66} for Ship 1. Number of panels: Solid line: 1568 on S_B, 6272 on S_F. Dashed line: 800 on S_B, 3200 on S_F. Dotted line: 392 on S_B, 1568 on S_F.

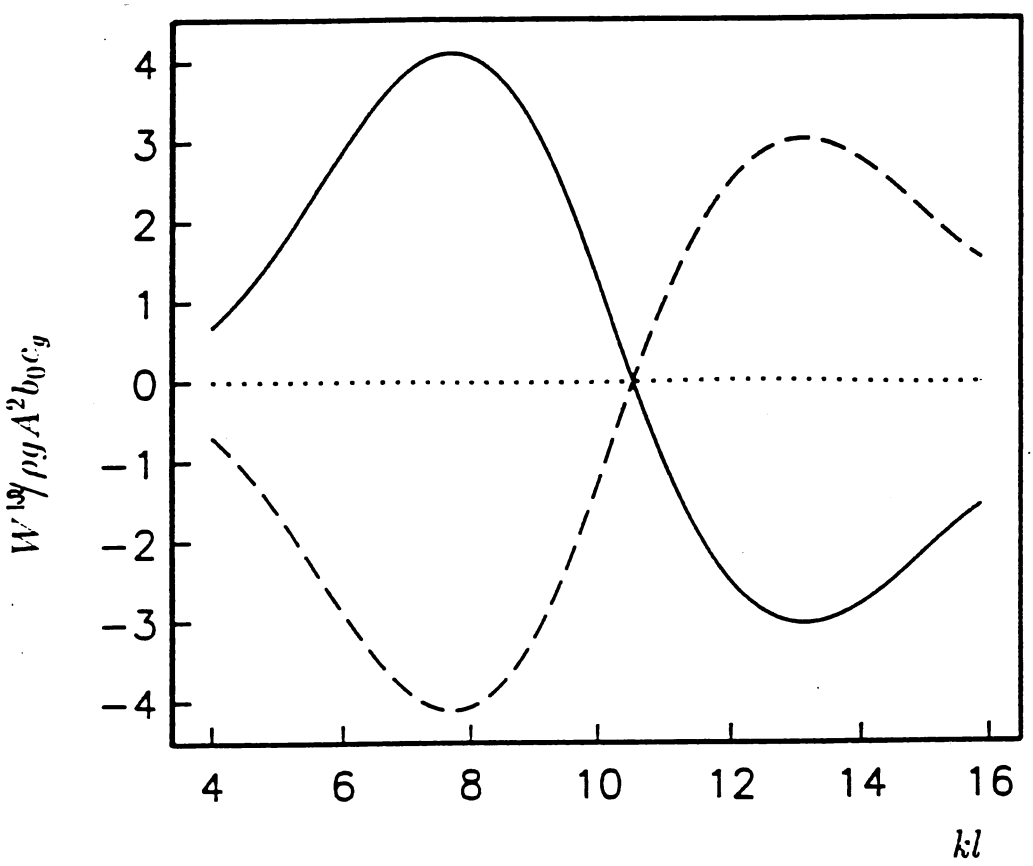

Figure 13: Energy flux $W^{1\Omega}$. Ship 1. Solid line: Far-field term. Dashed line: The remaining term. Dotted line: Total.

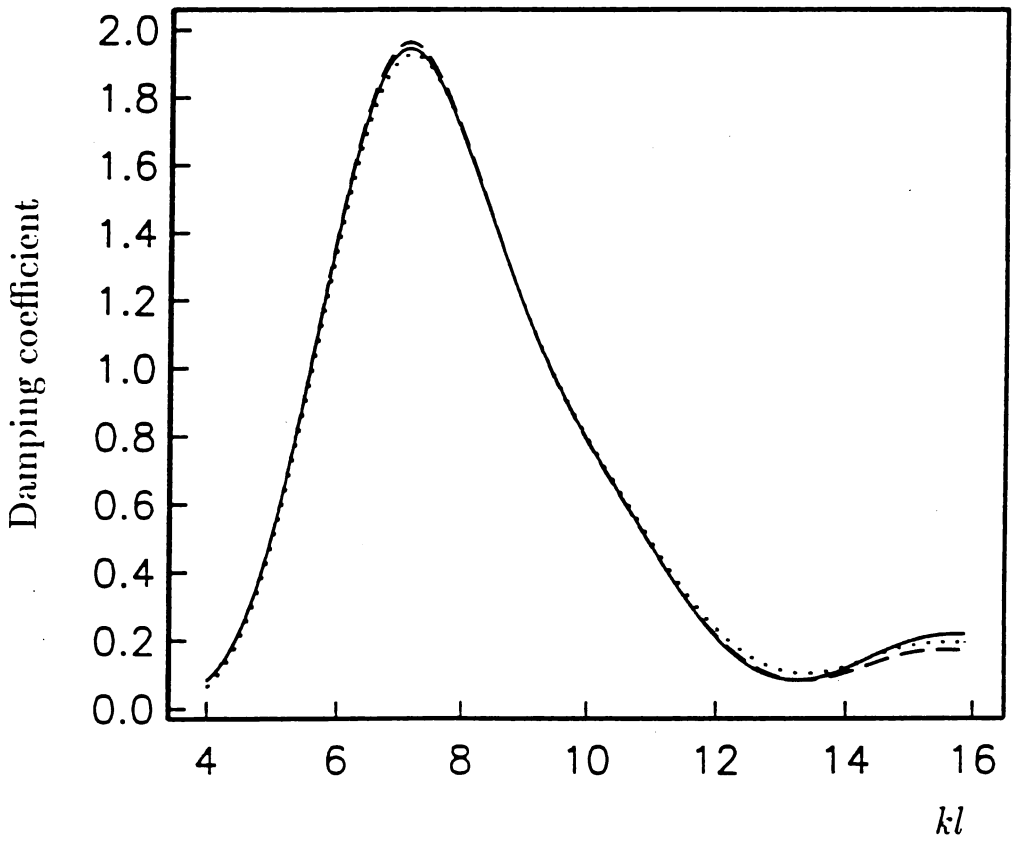

Figure 14: Comparison of the wave drift damping coefficients B_{11}, B_{16}, B_{66}. Ship 1. Distance s between the ship and the rotation axis is 100 shiplengths (the ship is almost translating). Head waves. Solid line: $B_{11}/\rho g A^2 b_0$, $B_{16}/\rho g A^2 b_0 sk$, $B_{66}/\rho g A^2 b_0 s^2 k$.

3 The potentials

We describe the incoming waves in the relative frame of reference by the potential

$$\Phi^I = Re[(Aig/\omega)\phi^I e^{i\sigma t}], \quad \phi^I = \frac{\cosh k(z+h)}{\cosh kh} e^{-ikR\cos(\beta-\theta)}, \tag{5}$$

where A, k and β denote respectively the amplitude, wavenumber and wave angle of the incoming waves and h the water depth. Furthermore,

$$\sigma = \omega - Uk\cos\beta - Vk\sin\beta \tag{6}$$

where

$$K = k\tanh kh \qquad K = \omega^2/g \tag{7}$$

The velocity potential Φ' describing the entire flow my be written by

$$\Phi' = \Phi + U\chi^U + V\chi^V + \Omega\chi^\Omega + \psi^{(2)} \tag{8}$$

where Φ denotes the linear wave potential being proportional to the wave amplitude and is due to the incoming, scattered and radiated waves, $U\chi^U + V\chi^V + \Omega\chi^\Omega$ the potential due to the flow generated by the body when there are no waves, and $\psi^{(2)}$ a time-averaged potential being proportional to the wave amplitude squared.

3.1 The wave potential Φ

We may write

$$\Phi = Re\Big(\frac{iAg}{\omega}\phi e^{i\sigma t}\Big) = Re\Big(\frac{iAg}{\omega}(\phi^0 + \tau(U)\phi^{1U} + \tau(V)\phi^{1V} + \tau(\Omega)\phi^{1\Omega})e^{i\sigma t}\Big) \tag{9}$$

We shall here be interested in the far-field. For ϕ^0 we have

$$\phi^0 - \phi^I = R^{-1/2}H^0(\theta)\frac{\cosh k^{1U}(z+h)}{\cosh k^{1U}h}e^{-ik^{1U}R} + O(1/R), \quad R\to\infty, \tag{10}$$

For the potentials due to U and V we find (see references [3], [9])

$$\phi^0 - \phi^I + \tau(U)\phi^{1U} = R^{-1/2}H^U(\theta)\frac{\cosh k^{1U}(z+h)}{\cosh k^{1U}h}e^{-ik^{1U}R} + O(1/R), \quad R\to\infty, \tag{11}$$

$$\phi^0 - \phi^I + \tau(V)\phi^{1V} = R^{-1/2}H^V(\theta)\frac{\cosh k^{1V}(z+h)}{\cosh k^{1V}h}e^{-ik^{1V}R} + O(1/R), \quad R\to\infty, \tag{12}$$

where

$$k^{1U} = k\Big(1 + \frac{2\tau(U)}{C_g(kh)}(\cos\theta - \cos\beta)\Big), \tag{13}$$

$$k^{1V} = k\Big(1 + \frac{2\tau(V)}{C_g(kh)}(\sin\theta - \sin\beta)\Big), \tag{14}$$

$$C_g(kh) = \tanh kh + \frac{kh}{\cosh^2 kh} \tag{15}$$

and $H^{U,V}$ denote far-field amplitudes of the potentials.

In the slow yaw-problem we obtain the potentials as follows, see references [11]–[13],

$$\phi^{1\Omega} = 2iK\frac{\partial^2\phi^0}{\partial K\partial\beta} + 2iK\frac{\partial^2\phi^0}{\partial K\partial\theta} + \phi^{13\Omega} \tag{16}$$

where $\phi_j^{13\Omega}$ satisfy

$$\phi^{13\Omega} = R^{-1/2}H^{13\Omega}(\theta)\frac{\cosh k(z+h)}{\cosh kh}e^{-ikR} + O(1/R), \quad R\to\infty \tag{17}$$

and $H^{13\Omega}$ denotes the far-field amplitude of $\phi^{13\Omega}$.

3.2 The potential $\psi^{(2)}$

The second order potential $\psi^{(2)}$ appears in the formulae for the second order fluid pressure, and for the mean force and moment always multiplied by the slow velocity $\mathbf{w}$. To leading order in Ω it is then sufficient to consider the boundary value problem for $\psi^{(2)}$ when $U = V = \Omega = 0$. The free surface condition for $\psi^{(2)}$ then reads

$$\frac{\partial\psi^{(2)}}{\partial z} = -\frac{1}{g}\overline{\frac{\partial}{\partial t}\nabla\Phi\cdot\nabla\Phi} + \frac{1}{g^2}\overline{\frac{\partial\Phi}{\partial t}\frac{\partial^3\Phi}{\partial z\partial t^2}} + \frac{1}{g}\overline{\frac{\partial\Phi}{\partial t}\frac{\partial^2\Phi}{\partial z^2}} = -\frac{A^2g}{2\omega}Im\Big(\phi^0\frac{\partial^2\phi^{0*}}{\partial z^2}\Big) \quad \text{at } z=0 \tag{18}$$

where a bar denotes time-average and a star complex conjungate.

The boundary condition at the body reads

$$\frac{\partial\psi^{(2)}}{\partial n} = -\mathbf{n}\cdot\overline{[(\tilde{\boldsymbol{\xi}}+\tilde{\boldsymbol{\alpha}}\times\boldsymbol{x})\cdot\nabla]\nabla\Phi} + \overline{(\tilde{\boldsymbol{\alpha}}\times\mathbf{n})\cdot[(d/dt)(\tilde{\boldsymbol{\xi}}+\tilde{\boldsymbol{\alpha}}\times\boldsymbol{x})-\nabla\Phi]} \tag{19}$$

where $\tilde{\boldsymbol{\xi}} = Re[(\xi_1,\xi_2,\xi_3)e^{i\sigma t}]$, $\tilde{\boldsymbol{\alpha}} = Re[(\xi_4,\xi_5,\xi_6)e^{i\sigma t}]$. Furthermore, $|\nabla\psi^{(2)}|\to 0$ for $R\to\infty$, $\partial\psi^{(2)}/\partial z = 0$ at $z=-h$.

The solution for $\psi^{(2)}$ may be obtained by an integral equation. The analysis below shows, however, that to find the mean force and moment, only the boundary conditions for $\psi^{(2)}$ are required, and not the complete solution for $\psi^{(2)}$. A complete discussion of the significance of $\psi^{(2)}$, and how to obtain the potential, is given in reference [8].

4 Formulae for the wave drift damping matix.

4.1

$$\frac{B_{11}}{\rho g A^2} = \frac{gk}{2\omega^2}\int_0^{2\pi}\left\{\frac{\cos\theta-\cos\beta}{C_g}\frac{\partial}{\partial k}\Big(C_g k|H^0|^2\Big)+\cos\theta|H^0|^2+C_g Re(H^0 H^{13U*})\right\}\cos\theta d\theta$$
$$+\ \frac{gk}{2\omega^2}C_g\cos\beta Re[S^{13U}] \tag{20}$$

where a star means complex conjungate and

$$S^{13U}=\sqrt{\frac{2\pi}{k}}e^{i\pi/4}H^{13U*}(\beta) \tag{21}$$

$$H^0 = H_7^0 + K(\xi_j^0/A)H_j^0 \tag{22}$$

$$H^{13U} = H_7^{13U} + \Big(K\xi_j^0 H_j^{13U} + 2k(\cos\beta-\cos\theta)\frac{\partial(K\xi_j^0)}{\partial K}H_j^0 + (K\xi_j^{1U} - k\cos\beta\xi_j^0)H_j^0\Big)/A \tag{23}$$

$$4\pi H_j^{13U} = \int_{S_B}[(2k\cos\theta\phi_{jK}^0-\psi_j^{1U})h_n^0+\frac{i}{K}\nabla h^0\cdot\mathbf{w}^U n_j]dS + i\int_{S_F}\phi_j^0 L_h(h^0,\chi^U)dS \tag{24}$$

$$4\pi H_7^{13U} = \int_{S_B}(2k\cos\theta\phi_{DK}^0-\psi_D^{1U})h_n^0 dS + i\int_{S_F}\phi_D^0 L_h(h^0,\chi^U)dS \tag{25}$$

$$\psi_j^{1U}=\phi_j^{1U}+2k\cos\beta\phi_{jK}^0, \qquad L_h(h,\chi)=2\nabla_h h\cdot\nabla_h\chi+h\nabla_h^2\chi \tag{26}$$

$$h^0=\frac{\sqrt{2\pi k}}{C_g(kh)}\Big(\tanh kh+1\Big)\Big(e^{k\zeta'}+e^{-k(\zeta'+2h)}\Big)e^{k(i\xi'\cos\theta+i\eta'\sin\theta)-i\pi/4} \tag{27}$$

$C_g(kh)$ is given by (15).

4.2

$$\frac{B_{21}}{\rho g A^2} = \frac{gk}{2\omega^2}\int_0^{2\pi}\left\{\frac{\cos\theta-\cos\beta}{C_g}\frac{\partial}{\partial k}\Big(C_g k|H^0|^2\Big)+\cos\theta|H^0|^2+C_g Re(H^0 H^{13U*})\right\}\sin\theta d\theta$$
$$+\ \frac{gk}{2\omega^2}C_g\sin\beta Re[S^{13U}] \tag{28}$$

4.3

$$\frac{B_{61}}{\rho g A^2} = \frac{g}{2\omega^2}Im\int_0^{2\pi}\left\{\frac{k(\cos\theta-\cos\beta)}{C_g}\frac{\partial}{\partial k}\Big(C_g H^0 H_\theta^{0*}\Big)+k\sin\theta H_k^0 H^{0*}+C_g H^0 H_\theta^{13U*}\right\}d\theta$$
$$+\frac{g}{2\omega^2}Im\left\{-\sin\beta\Big(\frac{1}{C_g}\frac{\partial}{\partial k}\Big(C_g k\Big)S^0+2k\frac{\partial S^0}{\partial k}\Big)-2\cos\beta S^{0'}+C_g S^{13U'}\right\}+\frac{g}{\omega^2}M_2 \tag{29}$$

where

$$S^0=\sqrt{\frac{2\pi}{k}}e^{i\pi/4}[H^0(\beta)]^*, \quad S^{0'}=\sqrt{\frac{2\pi}{k}}e^{i\pi/4}[H_\theta^0(\beta)]^*, \quad S^{13U'}=\sqrt{\frac{2\pi}{k}}e^{i\pi/4}[H_\theta^{13U}(\beta)]^* \tag{30}$$

$$M_2 = (\omega/gA^2)\int_{S_B+S_F}(\chi^V - y)\frac{\partial\psi^{(2)}}{\partial n}dS =$$
$$\frac{1}{2}Im\Big(-\int_{S_B}\mathbf{B}^0\cdot\mathbf{n}\nabla(\chi^V - y)\cdot\nabla\phi^{0*}dS + K\int_{C_B}(\chi^V - y)\mathbf{B}^0\cdot\mathbf{n}\phi^{0*}dl - \int_{S_F}(\chi^V - y)\phi^0\phi^{0*}_{zz}dS\Big) \tag{31}$$

$$\mathbf{B}^0 = [(\xi^0_1, \xi^0_2, \xi^0_3) + \boldsymbol{x}\times(\xi^0_4, \xi^0_5, \xi^0_6)]/A \tag{32}$$

4.4

$$\frac{B_{12}}{\rho g A^2} = \frac{gk}{2\omega^2}\int_0^{2\pi}\left\{\frac{\sin\theta - \sin\beta}{C_g}\frac{\partial}{\partial k}\Big(C_g k|H^0|^2\Big) + \sin\theta|H^0|^2 + C_g Re(H^0 H^{13V*})\right\}\cos\theta d\theta$$
$$+ \frac{gk}{2\omega^2}C_g\cos\beta Re[S^{13V}] \tag{33}$$

$$S^{13V} = \sqrt{\frac{2\pi}{k}}e^{i\pi/4}H^{13V*}(\beta) \tag{34}$$

$$H^{13V} = H_7^{13V} + \Big(K\xi^0_j H_j^{13V} + 2k(\sin\beta - \sin\theta)\frac{\partial(K\xi^0_j)}{\partial K}H^0_j + (K\xi^{1V}_j - k\sin\beta\xi^0_j)H^0_j\Big)/A \tag{35}$$

$$4\pi H_j^{13V} = \int_{S_B}[(2k\sin\theta\phi^0_{jK} - \psi^{1V}_j)h^0_n + \frac{i}{K}\nabla h^0\cdot\mathbf{w}^V n_j]dS + i\int_{S_F}\phi^0_j L_h(h^0, \chi^V)dS \tag{36}$$

$$4\pi H_7^{13V} = \int_{S_B}(2k\sin\theta\phi^0_{DK} - \psi^{1V}_D)h^0_n dS + i\int_{S_F}\phi^0_D L_h(h^0, \chi^V)dS \tag{37}$$

$$\psi^{1V}_j = \phi^{1V}_j + 2k\sin\beta\phi^0_{jK} \tag{38}$$

4.5

$$\frac{B_{22}}{\rho g A^2} = \frac{gk}{2\omega^2}\int_0^{2\pi}\left\{\frac{\sin\theta - \sin\beta}{C_g}\frac{\partial}{\partial k}\Big(C_g k|H^0|^2\Big) + \sin\theta|H^0|^2 + C_g Re(H^0 H^{13V*})\right\}\sin\theta d\theta$$
$$+ \frac{gk}{2\omega^2}C_g\sin\beta Re[S^{13V}] \tag{39}$$

4.6

$$\frac{B_{62}}{\rho g A^2} = \frac{g}{2\omega^2}Im\int_0^{2\pi}\left\{\frac{k(\sin\theta - \sin\beta)}{C_g}\frac{\partial}{\partial k}\Big(C_g H^0 H^{0*}_\theta\Big) - k\cos\theta H^0_k H^{0*} + C_g H^0 H^{13V*}_\theta\right\}d\theta$$
$$+\frac{g}{2\omega^2}Im\left\{\cos\beta\Big(\frac{1}{C_g}\frac{\partial}{\partial k}\Big(C_g k\Big)S^0 + 2k\frac{\partial S^0}{\partial k}\Big) - 2\sin\beta S^{0'} + C_g S^{13U'}\right\} - \frac{g}{\omega^2}M_1 \tag{40}$$

$$S^0 = \sqrt{\frac{2\pi}{k}}e^{i\pi/4}[H^0(\beta)]^*, \quad S^{0'} = \sqrt{\frac{2\pi}{k}}e^{i\pi/4}[H^0_\theta(\beta)]^*, \quad S^{13V'} = \sqrt{\frac{2\pi}{k}}e^{i\pi/4}[H^{13V}_\theta(\beta)]^* \tag{41}$$

$$M_1 = (\omega/gA^2)\int_{S_B+S_F}(\chi^U - x)\frac{\partial\psi^{(2)}}{\partial n}dS \tag{42}$$

(see also (31)).

4.7

$$\frac{B_{i6}\mathbf{i}_i}{\rho g A^2} = -(\mathbf{i}_i \frac{\partial}{\partial \beta} - \mathbf{k} \times \mathbf{i}_i) M_i$$
$$+\frac{1}{2}\int_0^{2\pi} Re\Big\{H^0(\theta)H^{1\Omega *}(\theta)\begin{pmatrix}\cos\theta\\ \sin\theta\end{pmatrix} - 2iH^0(\theta)\big[H^0_{\beta\theta}(\theta)+H^0_{\theta\theta}(\theta)\big]^*\begin{pmatrix}-\sin\theta\\ \cos\theta\end{pmatrix}\Big\}d\theta$$
$$+\frac{1}{2}Re\Big\{\sqrt{\frac{2\pi}{k}}e^{i\pi/4}\big[H^{1\Omega *}(\beta)\begin{pmatrix}\cos\beta\\ \sin\beta\end{pmatrix} - 2i\big[H^0_{\beta\theta}(\beta)+H^0_{\theta\theta}(\beta)\big]^*\begin{pmatrix}-\sin\beta\\ \cos\beta\end{pmatrix}\big]\Big\} \tag{43}$$

where

$$H^{1\Omega} = \frac{kC_g}{K}[2iK(H^0_{\beta K}+H^0_{\theta K})+H^{13\Omega}] + \frac{ik}{C_g}\frac{\partial C_g}{\partial k}(H^0_\beta + H^0_\theta) \tag{44}$$

$$H^{13\Omega} = H_7^{13\Omega} + K\Big[\Big(\xi_j^{1\Omega} + i\frac{\partial \xi_j^0}{\partial \beta} - 2i\frac{\partial^2(K\xi_j^0)}{\partial K \partial \beta}\Big)H_j^0 - 2i\frac{\partial(K\xi_j^0)}{\partial K}\frac{\partial H_j^0}{\partial \theta} + \xi_j^0 H_j^{13\Omega}\Big]/A \tag{45}$$

$$4\pi H_j^{13\Omega} = \int_{S_B}(2iK\phi^0_{jK}h^0_{\theta n} - \psi_j^{1\Omega}h_n^0 - i\nabla h^0\cdot \mathbf{w}^\Omega n_j)dS + i\int_{S_F}\phi_j^0 L_h(h^0,\chi^\Omega)dS \tag{46}$$

$$4\pi H_7^{13\Omega} = \int_{S_B}(2iK\phi^0_{DK}h^0_{\theta n} - \psi_D^{1\Omega}h_n^0)dS + i\int_{S_F}\phi_D^0 L_h(h^0,\chi^\Omega)dS \tag{47}$$

4.8

$$\frac{B_{66}}{\rho g A^2} = Im\Big\{\frac{\omega^2 M^c_{ij}\xi^{0*}_{i\beta}\xi^0_j}{\rho g A^2} + \frac{ic_{ij}(\xi^{0*}_{j\beta}\xi^{1\Omega}_i - \xi^{0*}_{i\beta}\xi^{1\Omega}_j)}{2\rho g A^2} - \frac{1}{2k}\int_0^{2\pi}(H^0_\beta(\theta)+H^0_\theta(\theta))H^{1\Omega *}(\theta)d\theta\Big\} \tag{48}$$

where c_{ij} denotes the usual hydrostatic matrix, which also may include mooring forces, and

$$M^c_{ij} = \begin{pmatrix} 0 & -M & 0 & MZ_G & 0 & -MX_G \\ M & 0 & 0 & 0 & MZ_G & -MY_G \\ 0 & 0 & 0 & 0 & 0 & 0 \\ -MZ_G & 0 & 0 & 0 & -I_{xy} & D_{yz} \\ 0 & -MZ_G & 0 & I_{xy} & 0 & -D_{xz} \\ MX_G & MY_G & 0 & -D_{yz} & D_{xz} & 0 \end{pmatrix} \tag{49}$$

M denotes the mass of the body, (X_G, Y_G, Z_G) the center of gravity, and

$$I_{xy} = \int_M z^2 dM, \quad D_{xz} = \int_M xz dM, \quad D_{yz} = \int_M yz dM. \tag{50}$$

5 Conservation of energy

The energy equation for translation has been described in the references [3], [4], [9]. Here we describe the case of a slow rotation, i.e.

$$\frac{d(E_b+E_f)}{dt} = -\int_{S_R}(p+\frac{1}{2}\rho\mathbf{v}^2+\rho gz)\mathbf{v}\cdot\mathbf{n}dS \tag{51}$$

expressing that the rate of change of kinetic plus potential energy of the floating body (E_b) and the fluid (E_f) inside the control surface S_R is equal to the energy flux at S_R. Let us consider the time-averaged energy equation, giving

$$W = -\overline{\int_{S_R}(p+\frac{1}{2}\rho\mathbf{v}^2+\rho gz)\mathbf{v}\cdot\mathbf{n}dS} - \overline{\frac{d(E_b+E_f)}{dt}} = W^0+\tau(\Omega)W^{1\Omega}+... \tag{52}$$

For W^0 and $W^{1\Omega}$ we find

$$\frac{W^0}{\rho g A^2 c_g} = -\frac{1}{C_g}\int_{S_R} Im\{\phi^0\phi_n^{0*}\}dS \tag{53}$$

$$\begin{aligned}
&\frac{W^{1\Omega}}{\rho g A^2 c_g} = \\
&\frac{1}{C_g}\Big[\int_{S_B} Re\{K\mathbf{B}^0\cdot\mathbf{n}(\phi_\beta^0 - i(\phi_7^{11\Omega}+K(\xi_{j\beta}^0/A)\phi_j^{11\Omega}))^*\}dS + \frac{1}{2}\frac{\partial}{\partial\beta}\int_{S_B} K|B_3^0|^2 n_3 dS \\
&-\frac{K}{\rho A^2}\frac{\partial}{\partial\beta}Re\{\xi_6^0(\xi_4^{0*}(\rho V_B X_B - m_b X_G)+\xi_5^{0*}(\rho V_B X_B - m_b Y_G))\} \\
&+\frac{K}{2\rho A^2}\frac{\partial}{\partial\beta}(|\xi_4^0|^2+|\xi_5^0|^2)(\rho V_B Z_B - m_b Z_G)+\frac{K^2}{2\rho A^2}\frac{\partial}{\partial\beta}(\xi_i^0\xi_j^{0*})M_{ij} \\
&-\int_0^{2\pi} Re\Big\{KH^0\Big[\frac{C_g}{K}\tilde{H}^{1\Omega}+\frac{i}{C_g}\frac{\partial C_g}{\partial k}H_\theta^0 - 2iC_g(H_{7K\beta}^0+K(\xi_{j\beta}^0/A)H_{jK}^0)\Big]^*\Big\}d\theta \\
&-Re\Big\{\sqrt{\frac{2\pi}{k}}e^{i\pi/4}K\Big[\frac{C_g}{K}\tilde{H}^{1\Omega}+\frac{i}{C_g}\frac{\partial C_g}{\partial k}H_\theta^0 - 2iC_g(H_{7K\beta}^0+K(\xi_{j\beta}^0/A)H_{jK}^0)\Big]^*\Big\} \\
&+K(-\frac{1}{k}+\frac{1}{C_g}\frac{\partial C_g}{\partial k})Re\{i\sqrt{\frac{2\pi}{k}}e^{i\pi/4}H_\theta^{0*}\}\Big]
\end{aligned} \tag{54}$$

where $c_g = \partial\omega/\partial k$, $B_3^0 = \mathbf{B}^0\cdot\mathbf{k}$ and $\tilde{H}^{1\Omega} = 2iK(H_{\beta K}^0+H_{\theta K}^0)+H_{13}$.

6 List of symbols

B_{ij} – wave drift damping matrix

$O - xyz$ – coordinate system in relative frame of reference

$\mathbf{i}, \mathbf{j}, \mathbf{k}$ – corresponding unit vectors

$U\mathbf{i} + V\mathbf{j} + \Omega\mathbf{k}$ – slow velocities of the body

Φ^I, ϕ^I – incoming wave potential

A, ω, k – amplitude, frequency, wavenumber of incoming waves

β – wave angle (between x-axis and wave direction)

g – acceleration of gravity (=9.81m/s)

$K = \omega^2/g$

h – water depth

$i = \sqrt{-1}$

$\sigma = \omega - Uk\cos\beta - Vk\sin\beta$ – encounter frequency

R and θ – defined by $x = R\cos\theta$, $y = R\sin\theta$

$\tau(U) = U\omega/g$, $\tau(V) = V\omega/g$, $\tau(\Omega) = \Omega/\omega$

Φ' – velocity potential

Φ – linear wave potential, proportional to A

χ^U, χ^V, χ^Ω – potentials due to slow velcities along x, y, z-directions

$\psi^{(2)}$ – time-averaged potential proportional to A^2

$\mathbf{w}^U = -\mathbf{i} + \nabla\chi^U$, $\mathbf{w}^V = -\mathbf{j} + \nabla\chi^V$, $\mathbf{w}^\Omega = -\mathbf{k} \times \boldsymbol{x} + \nabla\chi^\Omega$

$\mathbf{w} = U\mathbf{w}^U + V\mathbf{w}^V + \Omega\mathbf{w}^\Omega$

ϕ_K – partial derivative of ϕ with respect to K

∇_h – horizontal gradient

ϕ – potential

$\phi = \phi^0 + \tau(U)\phi^{1U} + \tau(V)\phi^{1V} + \tau(\Omega)\phi^{1\Omega}$ – perturbation expansion of ϕ

$\phi_j = \phi_j^0 + \tau(U)\phi_j^{1U} + \tau(V)\phi_j^{1V} + \tau(\Omega)\phi_j^{1\Omega}$
– perturbation expansion of ϕ_j, $j = 1, 2, ..., 6, D$

ψ_j^{1U}, ψ_j^{1V}, $\psi_j^{1\Omega}$ – potentials

ϕ_j^{11U}, ϕ_j^{11V}, $\phi_j^{11\Omega}$ – potentials

ϕ_j^{13U}, ϕ_j^{13V}, $\phi_j^{13\Omega}$ – potentials

ξ_j – response amplitude in mode number j, $j = 1, ..., 6$

ξ_j^0, ξ_j^{1U}, ξ_j^{1V}, $\xi_j^{1\Omega}$ – perturbations of ξ_j

$\mathbf{B}^0 = [(\xi_1^0, \xi_2^0, \xi_3^0) + \boldsymbol{x} \times (\xi_4^0, \xi_5^0, \xi_6^0)]/A$

n_j – generalized unit normal vector of the body

$L_h(\phi, \chi) = 2\nabla_h\phi \cdot \nabla_h\chi + \phi\nabla_h^2\chi$ – operator at $z = 0$

$H^0, H^U, H^V, H^{1U}, H^{1V}, H^{1\Omega}$ – far-field amplitudes

$H^{13U}, H^{13V}, H^{13\Omega}$ – far-field amplitudes

$H^0 = H_7^0 + K(\xi_j^0/A)H_j^0$

$H^{13U} = H_7^{13U} + \left(K\xi_j^0 H_j^{13U} + 2k(\cos\beta - \cos\theta)\frac{\partial(K\xi_j^0)}{\partial K}H_j^0 + (K\xi_j^{1U} - k\cos\beta\xi_j^0)H_j^0\right)/A$

$H^{13V} = H_7^{13V} + \left(K\xi_j^0 H_j^{13V} + 2k(\sin\beta - \sin\theta)\frac{\partial(K\xi_j^0)}{\partial K}H_j^0 + (K\xi_j^{1V} - k\sin\beta\xi_j^0)H_j^0\right)/A$

$H^{13\Omega} = H_7^{13\Omega} + K\left[\left(\xi_j^{1\Omega} + i\frac{\partial\xi_j^0}{\partial\beta} - 2i\frac{\partial^2(K\xi_j^0)}{\partial K\partial\beta}\right)H_j^0 - 2i\frac{\partial(K\xi_j^0)}{\partial K}\frac{\partial H_j^0}{\partial\theta} + \xi_j^0 H_j^{13\Omega}\right]/A$

$M_1 = (\omega/gA^2)\int_{S_B+S_F}(\chi^U - x)\frac{\partial\psi^{(2)}}{\partial n}dS$

$M_2 = (\omega/gA^2)\int_{S_B+S_F}(\chi^V - y)\frac{\partial\psi^{(2)}}{\partial n}dS$

k^{1U}, k^{1V} – wavenumbers

$C_g(kh) = \tanh kh + kh/\cosh^2(kh)$

S_B – wetted body surface,

S_F – free surface

p – pressure,

ρ – density of the fluid

F_x, F_y, M_z – horizontal drift force, yaw moment

$B(x)$ – local beam of ship 1

B_0 – beam of Ship 1 and TPS

l – ship length

$f_{jk} = a_{jk} + b_{jk}/i\sigma$ – added mass (real part) and damping (imaginary part)

f_{jk}^0, f_{jk}^{1U}, f_{jk}^{1V}, $f_{jk}^{1\Omega}$ – perturbations of f_{jk}

M – body mass

M_{ij} – body mass matrix

M_{ij}^c – matrix accounting for the Coriolis force

c_{ij} – hydrostatic coefficients

$W, W^0, W^{1\Omega}$ – energy fluxes

$\boldsymbol{X}_G$ – centre of gravity

$\boldsymbol{X}_B$ – centre of bouyancy

References

1) J. Grue & E. Palm (1985). Wave radiation and wave diffraction from a submerged body in a uniform current. J. Fluid Mech. 151.

2) J. Grue & E. Palm (1986). The influence of a uniform current on slowly varying forces and displacements. Appl. Ocean Res. 8.

3) J. Nossen, J. Grue & E. Palm (1991). Wave forces on three-dimensional floating bodies with small forward speed. J. Fluid Mech. 227.

4) J. Grue & E. Palm (1991). Currents and wave forces on ships and marine structures. In: Dynamics of marine vehicles and structures in waves, edited by W. G. Price, P. Temarel and A. J. Keane. Invited paper for the IUTAM symposium, Brunel University, Uxbridge, U.K. 1990.

5) J. Grue & E. Palm (1991). Wave loading on ships and platforms at a small forward speed. In: Proc. 10th Int. Conf. on Offshore Mech. and Arctic Engng. (OMAE), Eds. S. K. Chakrabarti et al.

6) J. Grue (1992). Drift force and drift moment on ships advancing with a small speed in oblique waves. Ship Tech. Res. 39.

7) Grue, J. & Palm, E. (1992). The mean yaw moment on floating bodies advancing with a forward speed in waves. Proc. 16th Int. Conf. on Offshore Structures (BOSS'92), London, Great Britain. Eds. M. H. Patel and R. Gibbins.

8) J. Grue & E. Palm (1993). The mean drift force and yaw moment on marine structures in waves and current. J. Fluid Mech. 250.

9) J. Grue & D. Biberg (1993). Wave forces on marine structures with small speed in water of restricted depth. Appl. Ocean Res. 15.

10) J. Grue & E. Palm (1994). A boundary element method for predicting wave forces on marine bodies with slow yaw-motion. Proc. 7th Int. Conf. Behaviour of Offshore Structures (BOSS '94), MIT, ed. C. Chryssostomidis, Vol. 2. Pergamon.

11) J. Grue (1996). Interaction between waves and slowly rotating floating bodies. In: Waves and Nonlinear Processes in Hydrodynamics. Edited by J. Grue, B. Gjevik and J. E. Weber. Kluwer Academic Publishers.

12) J. Grue & E. Palm (1996). Wave drift damping of floating bodies in slow yaw motion. J. Fluid Mech. 319.

13) S. Finne & J. Grue (1997). On the complete radiation-diffraction problem and wave-drift damping of marine bodies in the yaw mode of motion. J. Fluid Mech. 357.

14) J. Grue (1999). A note on the contributions to the wave-drift damping matrix from the time-averaged second order potential. Applied Ocean Res. 21.

Additional effect of external damping/mass/restoring

The symbols used here are defined in Chapter II and III and in reference 13. First we consider the equation of motion. Let the mass and restoring force matrices M_{ij} and c_{ij} contain external effects. Additional external damping may be written:

$$B_i^E = Re[-i\sigma b_{ij}^E(\xi_j^0 + \tau(U)\xi_j^{1U} + \tau(V)\xi_j^{1V} + \tau(\Omega)\xi_j^{1\Omega} + i\tau(\Omega)\xi_{j,\beta}^0)e^{i\sigma t}] \tag{1}$$

where $\sigma = \omega - kU\cos\beta - kV\sin\beta$. By using the relevant equations for the exciting and hydrodynamical damping forces, and (1) for B_i^E, we find that the equation of motion becomes, for zero speed and to leading order in $\tau(U)$, $\tau(V)$, $\tau(\Omega)$ respectively

$$(-\omega^2(M_{ij} + f_{ij}^0 - ib_{ij}^E/\omega) + c_{ij})\xi_j^0 = AX_i^0 \tag{2}$$

$$(-\omega^2(M_{ij} + f_{ij}^0 - ib_{ij}^E/\omega) + c_{ij})\xi_j^{1U} = AX_i^{1U} + [\omega^2 f_{ij}^{1U} - 2gk\cos\beta(M_{ij} + (Kf_{ij}^0)_{,K} - ib_{ij}^E/(2\omega))]\xi_j^0 \tag{3}$$

$$(-\omega^2(M_{ij} + f_{ij}^0 - ib_{ij}^E/\omega) + c_{ij})\xi_j^{1V} = AX_i^{1V} + [\omega^2 f_{ij}^{1V} - 2gk\sin\beta(M_{ij} + (Kf_{ij}^0)_{,K} - ib_{ij}^E/(2\omega))]\xi_j^0 \tag{4}$$

$$\begin{aligned}&(-\omega^2(M_{ij} + f_{ij}^0 - ib_{ij}^E/\omega) + c_{ij})\xi_j^{1\Omega} \\ &\quad = A(X_i^{1\Omega} + iX_{i,\beta}^0) + \omega^2[(f_{ij}^{1\Omega} - 2iM_{ij}^c)\xi_j^0 + 2i(M_{ij} + (Kf_{ij}^0)_{,K} - ib_{ij}^E/(2\omega))\xi_{j,\beta}^0]\end{aligned} \tag{5}$$

Next the expression for B_{66} is considered. The near-field contribution to B_{66} may be written

$$\frac{1}{2K}\int_{S_B} Re\{\phi_{,\beta}^{0*}\phi_{,n}^1 - \phi^1\phi_{,\beta n}^{0*} - \frac{\partial}{\partial\beta}(iK\mathbf{B}^0\cdot\mathbf{nw}\cdot\nabla\phi^{0*})\}dS = \frac{-1}{2\rho gA^2}Re[\ ] \tag{6}$$

where superscript 1 replaces superscript 1Ω and

$$\begin{aligned}Re[\ ] &= Re\{\xi_{i,\beta}^{0*}(A(iX_{i,\beta}^0 + X_i^1) + \omega^2 f_{ij}^0\xi_j^1 + \omega^2 f_{ij}^1\xi_j^0 + 2i\omega^2(Kf_{ij}^0)_{,K}\xi_{j,\beta}^0) - \xi_i^{1*}(AX_i^0 + \omega^2 f_{ij}^0\xi_j^0)_{,\beta}\} \\ &= Re\{\xi_{i,\beta}^{0*}(A(iX_{i,\beta}^0 + X_i^1) \\ &\qquad + \omega^2 f_{ij}^0\xi_j^1 + \omega^2 f_{ij}^1\xi_j^0 + 2i\omega^2(Kf_{ij}^0)_{,K}\xi_{j,\beta}^0) - \xi_j^{1*}(-\omega^2(M_{ji} - ib_{ji}^E/\omega) + c_{ji})\xi_{i,\beta}^0\} \\ &= Re\{\xi_{i,\beta}^{0*}(A(iX_{i,\beta}^0 + X_i^1) + \omega^2[f_{ij}^0\xi_j^1 + f_{ij}^1\xi_j^0 + 2i(Kf_{ij}^0)_{,K}]\xi_{j,\beta}^0 + (\omega^2 M_{ji} + i\omega b_{ji}^E - c_{ji})\xi_j^1)\}\end{aligned} \tag{7}$$

To obtain this result we have used (2). This means

$$\begin{aligned}&\frac{1}{2K}\int_{S_B} Re\{\phi_{,\beta}^{0*}\phi_{,n}^1 - \phi^1\phi_{,\beta n}^{0*} - \frac{\partial}{\partial\beta}(iK\mathbf{B}^0\cdot\mathbf{nw}\cdot\nabla\phi^{0*})\}dS \\ &= \frac{-1}{2\rho gA^2}Re\Big\{\xi_{i,\beta}^{0*}\{A(X_i^1 + X_{i,\beta}^0) - c_{ji}\xi_j^1 + \omega^2[(f_{ij}^0 + M_{ji} + ib_{ji}^E/\omega)\xi_j^1 + f_{ij}^1\xi_j^0 + 2i(Kf_{ij}^0)_{,K}\xi_{j,\beta}^0]\}\Big\}\end{aligned} \tag{8}$$

We now use (3) and find

$$\begin{aligned}&A(X_i^1 + iX_{i,\beta}^0) + \omega^2[f_{ij}^0\xi_j^1 + f_{ij}\xi_j^0 + 2i(Kf_{ij}^0)_{,K}\xi_{j,\beta}^0] = \\ &\qquad -(\omega^2 M_{ij} - i\omega b_{ij}^E - c_{ij})\xi_j^1 + 2i\omega^2 M_{ij}^c\xi_j^0 - i(2\omega^2 M_{ij} - i\omega b_{ij}^E)\xi_{j,\beta}^0\end{aligned} \tag{9}$$

This means that the term on the right of (8) becomes

$$Re\Big\{\xi_{i,\beta}^{0*}\{[(c_{ji} - c_{ij}) + \omega^2(M_{ij} - M_{ji}) - i\omega(b_{ij}^E + b_{ji}^E)]\xi_j^1 - 2i\omega^2 M_{ij}^c\xi_j^0 + i[2\omega^2 M_{ij} - i\omega b_{ij}^E]\xi_{j,\beta}^0\}\Big\}/(2\rho gA^2) \tag{10}$$

The term (10) determines the near-field contribution to B_{66}. The expression for the far-field contribution to B_{66} remains unchanged.

III. WAVE DRIFT DAMPING WITH WAMITUIO PANEL PROGRAM. MODULE INTEGRATED IN WAMIT

Wave drift damping with WAMITUIO
Panel program. Module integrated in WAMIT

QUANTITIES EVALUATED BY WAMITUIO

ADDED-MASS AND DAMPING COEFFICIENTS (IOPTN(1) = 1):

See eqs. (74)–(77), Chapter I.

Zero speed:

$$\overline{A}^0_{ij} = \frac{A^0_{ij}}{\rho L^m}, \overline{B^0}_{ij} = \frac{B^0_{ij}}{\rho L^m \omega}$$

Derivative with respect to $K = \omega^2/g$:

$$\text{REAL/IMAGINARY PART OF } \overline{f}^0_{ij,K} = \frac{f^0_{ij,K}}{\rho L^m}$$

Perturbation due to speed along the x-axis:

$$\text{REAL/IMAGINARY PART OF } \overline{f}^{1U}_{ij} = \frac{f^{1U}_{ij}}{\rho L^m}$$

Perturbation due to speed along the y-axis:

$$\text{REAL/IMAGINARY PART OF } \overline{f}^{1V}_{ij} = \frac{f^{1V}_{ij}}{\rho L^m}$$

Perturbation due to rotation about the z-axis:

$$\text{REAL/IMAGINARY PART OF } \overline{f}^{1\Omega}_{ij} = \frac{f^{1\Omega}_{ij}}{\rho L^m}$$

where $m = 3$ for $i, j = 1, 2, 3$, $m = 4$ for $i = 1, 2, 3, j = 4, 5, 6$ or $i = 4, 5, 6, j = 1, 2, 3$, and $m = 5$ for $i, j = 4, 5, 6$.

EXCITING FORCES (IOPTN(2,3) = 1):

See eqs. (63)–(64), Chapter I.

Zero speed:

$$\overline{X}^0_i = \frac{X^0_i}{\rho g A L^m}$$

Derivative with respect to the wave angle β:

$$\overline{X}^0_{i,\beta} = \frac{X^0_{i,\beta}}{\rho g A L^m}$$

Perturbation due to speed along the x-axis:

$$\overline{X}^{1U}_i = \frac{X^{1U}_i}{\rho g A L^m}$$

Perturbation due to speed along the y-axis:

$$\overline{X}^{1V}_i = \frac{X^{1V}_i}{\rho g A L^m}$$

Perturbation due to rotation about the z-axis:

$$\overline{X}^{1\Omega}_i = \frac{X^{1\Omega}_i}{\rho g A L^m}$$

where $m = 2$ for $i = 1, 2, 3$ and $m = 3$ for $i = 4, 5, 6$.

BODY MOTIONS IN WAVES (IOPTN(4) = 1):

See eqs. (16) and (78)–(93), Chapter I.

Zero speed:

$$\overline{\xi}^0_i = \frac{\xi^0_i}{A}$$

Derivative with respect to the wave angle β:

$$\overline{\xi}^0_{i,\beta} = \frac{\xi^0_{i,\beta}}{A}$$

Perturbation with respect to speed along the x-axis:

$$\overline{\xi}^{1U}_i = \frac{\xi^{1U}_i}{A}$$

Perturbation with respect to speed along the y-axis:

$$\overline{\xi}^{1V}_i = \frac{\xi^{1V}_i}{A}$$

Perturbation with respect to rotation about the z-axis:

$$\overline{\xi}_i^{1\Omega} = \frac{\xi_i^{1\Omega}}{A}$$

PRESSURE AT CENTROIDS OF INPUT PANELS (IOPTN(5) = 1):

$$P = P^0 + \tau(U)P^{1U} + \tau(V)P^{1V} + \tau(\Omega)P^{1\Omega}$$

The pressure components are complex amplitudes. For $\tau(U)$ $\tau(V)$ $\tau(\Omega)$, see eq. (5), Chapter I.

Zero speed:

$$\overline{P}^0 = \frac{P^0}{\rho g A}$$

Perturbation with respect to speed along the x-axis:

$$\overline{P}^{1U} = \frac{P^{1U}}{\rho g A}$$

Perturbation with respect to speed along the y-axis:

$$\overline{P}^{1V} = \frac{P^{1V}}{\rho g A}$$

Perturbation with respect to rotation about the z-axis:

$$\overline{P}^{1\Omega} = \frac{P^{1\Omega}}{\rho g A}$$

PRESSURE/FREE SURFACE ELEVATION AT FIELD POINTS (IOPTN(6) = 1):

$$P = P^0 + \tau(U)P^{1U} + \tau(V)P^{1V} + \tau(\Omega)P^{1\Omega}$$

The components of pressure/elevation are complex amplitudes.

Zero speed:

$$\overline{P}^0 = \frac{P^0}{\rho g A}$$

Perturbation with respect to speed along the x-axis:

$$\overline{P}^{1U} = \frac{P^{1U}}{\rho g A}$$

Perturbation with respect to speed along the y-axis:

$$\overline{P}^{1V} = \frac{P^{1V}}{\rho g A}$$

Perturbation with respect to rotation about the z-axis:

$$\overline{P}^{1\Omega} = \frac{P^{1\Omega}}{\rho g A}$$

FLUID VELOCITY VECTOR AT FIELD POINTS (IOPTN(7)):

Same output as for zero speed.

MEAN HORIZONTAL DRIFT FORCE AND YAW-MOMENT (IOPTN(8) = 1):

See eqs. (1)–(2), Chapter II.

Zero speed:

$$\overline{F}_{1,2} = \frac{F_{1,2}}{\rho g A^2 L}, \quad \overline{M}_6 = \frac{M_6}{\rho g A^2 L^2}$$

Wave-drift damping matrix:

$$\overline{B}_{ij} = \frac{B_{ij}}{\rho g A^2 L}, i = 1, 2, \quad \overline{B}_{6j} = \frac{B_{6j}}{\rho g A^2 L^2}$$

MEAN ENERGY FLUX (IOPTN(8) = 1):

$$W = W^0 + \tau(U) W^{1U} + \tau(V) W^{1V} + \tau(\Omega) W^{1\Omega}$$

For $\tau(U)$ $\tau(V)$ $\tau(\Omega)$, see eq. (5), Chapter I.

$$\overline{W} = \frac{W}{\rho g A^2 c_g L}$$

where c_g denotes group velocity.

INPUT TO THE PROGRAM

The control parameter **IWADD** is used in the WAVE DRIFT DAMPING VERSION of WAMIT5.3 in addition to the standard control parameters.

IWADD = 1 means that effect of slow motions in the three horizontal modes of motion are included, and that the complete wave drift damping matrix and related quantities are evaluated. IWADD = 1 is default value in this version of WAMIT.

IWADD = 0 means zero slow speed, with WAMIT kept in the original form.
IWADD = 0 may be specified as the last parameter in 'config.wam'. It is not necessary to specify IWADD unless the user wants to employ the original zero speed version of WAMIT.

The input files are:
xxxx.GDF
xxxx.POT
xxxx.FRC
xxxx.FDF
These input files may be specified in fnames.wam.

The GEOMETRIC DATA FILE (.GDF) is the same as for WAMIT5.3

The POTENTIAL CONTROL FILE (.POT) is the same as for WAMIT5.3

The FORCE CONTROL FILE (.FRC) is the same as for WAMIT5.3

The following restrictions apply for IWADD = 1:
It is not possible with additional walls.
NBODY must be 1.
ISOR must be 1.
IRR must be zero.
IDIFF can be either 1 or -1.
ISOLVE must be 0 or 1.
ISCATT must be 0.
IOPTN(5) can take the values 0,1,2,3. For 2 and 3 the velocity field with zero speed is obtained.
IOPTN(6) cannot not be equal to 2.
IOPTN(7) can be equal to 0 or 2. In the latter case the velocity field with zero speed is computed.
IOPTN(8) cannot be equal to 2.
IOPTN(9) must be equal to zero.

The FREE SURFACE DATA FILE (.FDF).

The xxxx.FDF file specifies the discretization of the free surface with format as for WAMIT5.3S.

A group of four vertices, numbered in a COUNTER-CLOCKWISE sense when viewed from the fluid domain, is used to identify a panel. This is the same as for the xxxx.GDF-file.

The parameters PARTS and NPF are read as dummy variables and are NOT used.
The .FDF file is not assumed if IWADD = 0.

SUGGESTED DISCRETIZATION OF THE FREE SURFACE

The free surface integrands in the integral equations converge quickly with respect to the radial coordinate. The free surface contribution to some of the quantities have, however, somewhat slow convergence with respect to the distance from the geometry. A discretization with panel areas being proportional to the radial distance squared is recommended. It is suggested that the outer discretization radius, R_{out}, is chosen according to:

$R_{out} = L$ for a ship with length L.

$R_{out} = 2L$ for a platform with distance L between the columns.

$R_{out} = 6L$ for a vertical cylinder/sphere with radius L.

AUTOMATIC GRIDDING OF THE FREE SURFACE

The program may also be run with the same input as for the zero speed program WAMIT5.3, without specifying a discretization of the free surface. The program then checks if there is no xxxx.FDF-file, and, if so, generates a discretization of the free surface and writes this to an xxxx.FDF-file, the latter to be specified in fnames.wam file.

The automatic discretization routine is not intended to be general and has curently the following restrictions:

One intersection between the geometry and free surface is assumed.

The following symmetries may be used: Symmetry about the x-axis. Symmetry about the x- and y-axes.